

Response to Reviewer 1's comments on "Microbial dynamics in a High-Arctic glacier forefield: a combined field, laboratory, and modelling approach."

We are thankful for the helpful comments of the reviewer in the third round of revisions. We have addressed all final concerns that were raised.

The authors have made a sincere and detailed effort to improve the manuscript by addressing comments made in the earlier reviews. I am still wary about the use of measurements at 25°C with soils conditioned to 5°C, but can accept its necessity for the present study. The open nature of the review process offers readers with the inclination an opportunity to view the arguments for and against the use of 25°C temperatures.

Sequencing 16S rRNA genes to parameterize the model.

I still have problems here. It is assumed that shifts in the absolute quantities of different functional/taxonomic groups are meaningfully represented by DNA extracted from varying quantities of samples, amplified and sequenced to an unstated but incomplete depth, used to generate relative abundance profiles of sequence libraries which may differ in read number, and in any case are based upon sequences from a locus which has variable numbers of copies per bacterial genome, a source of variation which is known to be related to ecological traits important in glacier forefield successional processes and itself recapitulated within the data. Specifically:

A. L179: Thanks for updating the details here, but I have concerns over "5-10 grams of sample" being used for DNA extraction.

1. If this is the case, the statement DNA was extracted by "MoBio PowerSoil® DNA Isolation Kit and by following the instruction manual cannot be the case. This kit processes samples in 2 mL tubes for bead beating. The standard recommendation from the manufacturer is for 250 mg samples (and I have had no problems with getting enough DNA from forefield soils for amplicon sequencing from 250 mg using the standard protocol.) The key point is that 5-10 grams would not fit, and any more than 250-500 mg clogs the bead beating tube to the point that extraction efficiency is reduced, making using more sample counterproductive, so I think there's a mistake here. Did the authors actually use a PowerMax kit which can process up to 10 g of sample in a very different format, or modify the powersoil protocol to pool extracts from multiple 250 mg extracts? This may seem a trivial detail, but establishing how you extracted the DNA is important to establish whether the sequencing data have any relation to the soil community.

We would like to thank the referee for this important point. The "MoBio PowerSoil® DNA Isolation Kit" as referenced in the manuscript was indeed a mistake. We have corrected this to "PowerMax® Soil DNA Isolation Kit" in the revised manuscript (line 178).

2. So, some of your samples were 5 grams and some were 10 grams? How did you account for up to two fold variation in sample mass, with the implications for the total biomass in the tube, and furthermore the extractable biomass as a result of variation in extraction efficiency from the consequently variable ratios and mixing in volumes of sample, beads, buffer and tube during bead beating?

The referee correctly points out that by using 5-10g for the DNA extraction there could have been up to two fold variation in sample mass per tube, resulting in variation in the total biomass in the tube. It is worth noting that variation in biomass in each extraction tube also occurs regardless of sample volume, due to natural variability in cell biomass abundance along the chronosequence (see Table 2).

In an effort to normalize between samples with varying amounts of biomass following extraction, DNA was diluted to equimolar concentrations, so that all samples contained 7.0 ng of DNA prior to amplification. Then, following amplification, all amplicons were normalized to the same concentration (9.0 ng) before sequencing. This information has been added to the revised manuscript (lines 180-190).

B. L193-200: To establish the depth of sequencing and how many reads were there per barcode, and was the depth of sequencing? In other words, how can the reader be assured that your sequencing effort meaningfully describes the community, and that your relative abundance profiles are from roughly equivalent (or rarefied) numbers of reads. This matters because you are using proportional data from sequencing libraries to make estimations of absolute contributions to the soil community your model describes.

The final OTU table contained between 2329-43269 reads for each sample. The varying sequence coverage among samples was adjusted by normalizing the OTU matrix to the same total abundance of sequences for each sample (2329) using the command `normalize_table.py` in QIIME. Rarefaction curves (below) show incomplete sample depth. However, despite shortcomings of the depth of sequencing, the taxonomic information provides a useful snapshot with which to support and complement the modelling exercise and does not affect the major conclusions of the study.

This information has been included and discussed in the revised manuscript (lines 200-207, 619-623 and 674-675) and the rarefaction plot has been included in the Supplementary Material (Fig. S6) for transparency.

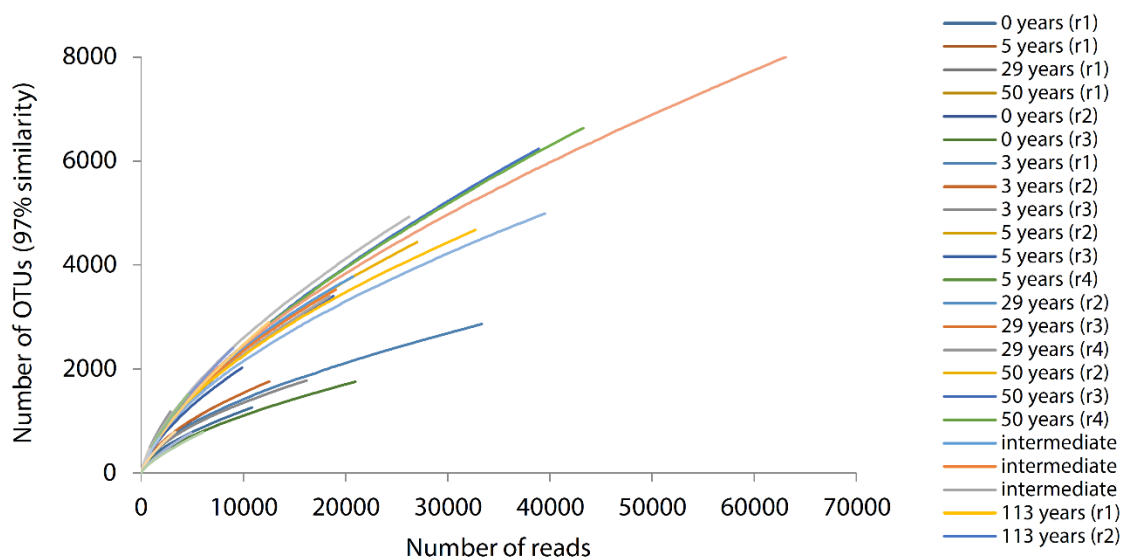


Fig. S6. Rarefaction curves for sequencing.

C. From the taxonomic profiles I see important changes in the community's composition and configuration which mirror other work on transitions between

oligotrophic and copiotrophic taxa in a variety of glacier chronosequences. That transition is associated with changes in ribosomal RNA gene copy number per genome. There are bioinformatic means of normalising this variation in rRNA copy number, for example CopyRighter (DOI: 10.1186/2049-2618-2-11).

We thank the reviewer for bringing up this concern. Following this, we have implemented CopyRighter on some taxa, and results were not different. However, implementing on all taxa and re-classifying for the functional groups as defined by the model is not possible at this stage. Thus, as the reviewer has suggested below, we have added a caveat to the discussion to state that absolute numbers should be treated with caution due to the differential extractability of DNA from different organisms and variation in rDNA copy number (lines 619-622 and 668-670).

I would hope the authors can state succinctly the measures taken to address problems A and B, and caveat their discussion to address concern C. This would serve to improve this paper, and perhaps consideration of these issues will help the other paper mentioned in their response which will probably rely on this 16S data a central pillar. As a general thought, for future endeavours and considering the broad taxonomic resolution desired by the authors to inform their model, I feel there are more appropriate tools for this job. If DNA based analyses were needed, qPCR or FISH would have provided data more closely linked to microbial abundance. Otherwise, PLFA would have provided taxonomically-informed estimates of contributions to biomass.

We hope that the above has satisfied the reviewer's concerns regarding the genomic data component of the study.

Minor comments.

L180: At this point it is not isolated rDNA; it will be community genomic DNA, from which you will specifically amplify bacterial 16S ribosomal RNA genes (rDNA itself is a common misnomer too, by the way: the gene product is rRNA, hence rRNA gene)

Corrected (line 181)

L183: dNTPs

Corrected (line 184)

Accession numbers: Hopefully NCBI will have returned the numbers soon.

Sequence data is available on NCBI under project ID PRJNA341831 (lines 205-207), and individual accession numbers are provided in the Supplementary Information.

Accession nr.	Sample Name	Soil Age
SAMN05729451	S132101a	0
SAMN05729452	S132102a	0
SAMN05729453	S131101a	0
SAMN05729454	S132301a	29
SAMN05729455	S132303a	29
SAMN05729456	S132302a	29
SAMN05729457	S131301a	29
SAMN05729458	S133301a	29

SAMN05729459	S132503a	50
SAMN05729460	S132501a	50
SAMN05729461	S132502a	50
SAMN05729462	S131501a	50
SAMN05729463	S133501a	50
SAMN05729464	S132603a	113
SAMN05729465	S132602a	113
SAMN05729466	S132601a	113

Response: “ Assuming that predation rates and dormancy are the same on all functional groups (as is defined in SHIMMER),” I advise caution in making that assumption as these traits are varied across the breadth of soil microbiota.

We acknowledge that the assumption of equal predation/dormancy rates between functional groups is a simplification, but it is a necessary assumption for the purpose of model-16S comparison using this method. We are thankful to the reviewer for suggesting the use of other techniques (qPCR, FISH, PLFA) for future endeavours.

1 **Microbial dynamics in a High-Arctic glacier forefield: a combined field, laboratory, and modelling**
2 **approach.**

3 James A. Bradley ^{1,2}, Sandra Arndt ², Marie Šabacká ¹, Liane G. Benning ^{3,4}, Gary L. Barker ⁵, Joshua
4 J. Blacker ³, Marian L. Yallop ⁵, Katherine E. Wright ¹, Christopher M. Bellas ¹, Jonathan Telling ¹, Martyn
5 Tranter ¹, Alexandre M. Anesio ¹

6
7 ¹ Bristol Glaciology Centre, School of Geographical Sciences, University of Bristol, BS8 1SS, UK

8 ² BRIDGE, School of Geographical Sciences, University of Bristol, BS8 1SS, UK

9 ³ School of Earth and Environment, University of Leeds, LS2 9JT, UK

10 ⁴ GFZ, German Research Centre for Geosciences, 14473 Potsdam, Germany

11 ⁵ School of Biological Sciences, University of Bristol, BS8 1SS, UK

12

13 Corresponding author: James A. Bradley, email: j.bradley@bristol.ac.uk

14

15 **Abstract:** Modelling the development of soils in glacier forefields is necessary in order to assess how
16 microbial and geochemical processes interact and shape soil development in response to glacier
17 retreat. Furthermore, such models can help us predict microbial growth and the fate of Arctic soils in an
18 increasingly ice-free future. Here, for the first time, we combined field sampling with laboratory analyses
19 and numerical modelling to investigate microbial community dynamics in oligotrophic proglacial soils in
20 Svalbard. We measured low bacterial growth rates and growth efficiencies (relative to estimates from
21 Alpine glacier forefields), and high sensitivity to soil temperature (relative to temperate soils). We used
22 these laboratory measurements to inform parameter values in a new numerical model and significantly
23 refined predictions of microbial and biogeochemical dynamics of soil development over a period of
24 roughly 120 years. The model predicted the observed accumulation of autotrophic and heterotrophic
25 biomass. Genomic data indicated that initial microbial communities were dominated by bacteria derived
26 from the glacial environment, whereas older soils hosted a mixed community of autotrophic and
27 heterotrophic bacteria. This finding was simulated by the numerical model, which showed that active
28 microbial communities play key roles in fixing and recycling carbon and nutrients. We also demonstrated
29 the role of allochthonous carbon and microbial necromass in sustaining a pool of organic material,
30 despite high heterotrophic activity in older soils. This combined field, laboratory and modelling approach
31 demonstrates the value of integrated model-data studies to understand and quantify the functioning of
32 the microbial community in an emerging High-Arctic soil ecosystem.

33

34 **Key words**

35 Glacier forefield

36 Microbial dynamics

37 Soil development

38 Numerical modelling

39 Integrated field-laboratory-modelling

40 SHIMMER

41

42 **1. Introduction**

43 Polar regions are particularly sensitive to anthropogenic climate change (Lee, 2014) and have
44 experienced accelerated warming in recent decades (Johannessen et al., 2004; Serreze et al., 2000;
45 Moritz et al., 2002). The response of terrestrial Polar ecosystems to this warming is complex, and
46 research to understand the response of terrestrial ecosystems in high latitudes to environmental change
47 is of increasing importance. A visible consequence of Arctic warming is the large-scale retreat of glacier
48 and ice cover (ACIA, 2005; Paul et al., 2011; Staines et al., 2014; Dyurgerov and Meier, 2000). From
49 underneath the ice, a new terrestrial biosphere emerges, playing host to an ecosystem which may exert
50 an important influence on biogeochemical cycles, and more specifically atmospheric CO₂
51 concentrations and associated climate feedbacks (Dessert et al., 2003; Anderson et al., 2000;
52 Smittenberg et al., 2012; Berner et al., 1983).

53

54 Numerous studies have attempted to characterize the physical and biological development of recently
55 exposed soils using a chronosequence approach, whereby a transect perpendicular to the retreating
56 ice snout represents a time sequence with older soils at increasing distance from the ice snout (Schulz
57 et al., 2013). We have recently shown that microbial biomass and macronutrients (such as carbon,
58 phosphorus and nitrogen) can accumulate in soils over timescales of decades to centuries (Bradley et
59 al., 2014). In such pristine glacial forefield soils the activity of microbial communities is thought to be
60 responsible for this initial accumulation of carbon and nutrients. Such an accumulation facilitates
61 colonization by higher order plants, leading to the accumulation of substantial amounts of organic
62 carbon (Insam and Haselwandter, 1989). However, organic carbon may also be derived from
63 allochthonous sources such as material deposited on the soil surface (from wind, hydrology,
64 precipitation and ornithogenic sources) and ancient organic pools derived from under the glacier (Schulz
65 et al., 2013). Nevertheless, the relative significance of allochthonous and autochthonous sources of
66 carbon to forefield soils, as well as their effect on ecosystem behaviour are so far still poorly understood
67 (Bradley et al., 2014). Moreover, cycling of bioavailable nitrogen (which is derived from active nitrogen-
68 fixing organisms, allochthonous deposition, and degradation of organic substrates) and phosphorus
69 (liberated from the weathering of minerals and decomposition of organic substrates) are similarly poorly
70 quantified.

71

72 Several studies have observed shifts in the microbial community inhabiting pro-glacial soils of various
73 ages (Zumsteg et al., 2012; Zumsteg et al., 2011). This was expressed in increasing rates of autotrophic
74 and bacterial production with soil age (Schmidt et al., 2008; Zumsteg et al., 2013; Esperschütz et al.,
75 2011; Frey et al., 2013) and the overall decline in quality of organic substrates in older soils (Goransson
76 et al., 2011; Insam and Haselwandter, 1989). However, current evidence is limited to mostly descriptive
77 approaches, which may be challenging to interpret due to inherent difficulties in disentangling interacting
78 microbial and geochemical processes across various temporal and spatial scales. Furthermore, the
79 inherent heterogeneity of glacial forefield soils makes the development of a single conceptual model
80 that fits all challenging. Accordingly, pro-glacial biogeochemical processes that dominate such systems

81 remain poorly quantified and highly under-explored. This current lack of understanding limits our ability
82 to predict the future evolution of these emerging landscapes and the potential consequences on global
83 climate. Numerical models present an opportunity to expand our knowledge of glacier forefield
84 ecosystems by analytically testing the hypotheses that arise from observations, extrapolating,
85 interpolating and budgeting processes, rates and other features to explore beyond the possibility of
86 empirical observation (Bradley et al., 2016). With such a model we can then also explore the sensitivity
87 and resilience of these ecosystems to environmental change.

88

89 Here, we have combined field observations, with laboratory incubations and elemental measurements
90 as well as genomic analyses and used these in a numerical model to investigate the development of
91 soils in a glacial forefield. The present study forms an important part of the integrated and iterative
92 model-data approach outlined in the model description and testing (Bradley et al, 2015) whereby initial
93 model development was informed by decades of empirical research, new data and laboratory
94 experiments (presented here) are used to refine and inform model simulations, and so forth. With this
95 data we refined some model parameters in the recently developed **Soil biogeocHemical Model for**
96 **Microbial Ecosystem Response** (SHIMMER 1.0; Bradley et al. (2015)) model and applied this to the
97 emerging forefield of the Midtre Lovénbreen glacier in Svalbard. Pioneer soils in the High-Arctic and
98 Antarctica, such as the Midtre Lovénbreen forefield, are ideal sites to test this field-laboratory-model
99 approach due to the lack of vegetation during initial stages of soil development, as the presence of
100 vegetation would obscure the microbial community dynamics and considerably alter the physical
101 properties of the soil (Brown and Jumpponen, 2014; Ensign et al., 2006; King et al., 2008; Kastovska
102 et al., 2005; Schutte et al., 2009; Duc et al., 2009). The model development was informed by decades
103 of empirical research on glacier forefield soils, and has already been tested and validated using
104 published datasets from the Damma Glacier in Switzerland and the Athabasca Glacier in Canada. A
105 thorough sensitivity analysis highlighted the most important parameters to constrain in order to make
106 further predictions more robust. All our model parameter values are specific to individual, local model
107 conditions and inherently contain necessary model simplifications, abstractions and assumptions.
108 Nevertheless, our earlier sensitivity analyses revealed the following highly sensitive key parameters as
109 the most important to constrain through measurements: the maximum heterotrophic growth rate (I_{maxH}),
110 the bacterial growth efficiency (BGE, parameter Y_H) and the temperature response (Q_{10}).

111

112 Therefore, in this current study, we combined detailed field measurements with specifically designed
113 laboratory experiments and quantified values for these three parameters with a specific set of soils from
114 for the Midtre Lovénbreen forefield. The laboratory experiments and measurements were conducted
115 with the objective to better constrain these sensitive parameters. We then ran model simulations in
116 order to explore the ranges of model output and refine model predictions compared to the previous
117 range identified in Bradley et al (2015). Next, we examined model output to explore the microbial and
118 biogeochemical dynamics of recently exposed soils in the Midtre Lovénbreen catchment and evaluate
119 two main hypotheses. First, we tested the hypothesis that microbial biomass in recently exposed soils
120 accumulates due to *in situ* bacterial growth and activity. It is commonly observed in glacier forefields

121 that microbial biomass accumulates with increasing soil age following exposure (Bernasconi et al.,
122 2011; Schulz et al., 2013; Bradley et al., 2014). This study provides a new quantitative and process-
123 focused approach to examine *in situ* growth in pioneer ecosystems, and assess the role of different
124 functional groups in biomass accumulation. Second, we tested the hypothesis that carbon fluxes in very
125 recently exposed soils are low, and are dominated by (abiotic) deposition of allochthonous substrate,
126 whereas carbon fluxes are high in older soils due to increased microbial (biotic) activity (such as
127 microbial growth, respiration and cell death). Increased soil carbon fluxes with soil age have been linked
128 to microbial activity from the forefield of the Damma Glacier, Switzerland (Smittenberg et al., 2012;
129 Guelland et al., 2013b). With this combined model, field and lab study, we were able to estimate carbon
130 fluxes between ecosystem components with daily resolution, and provide new insight into the interplay
131 of processes that contribute to net ecosystem production and soil organic carbon stocks in a High-Arctic
132 system.

133

134 **2. Methods**

135 **2.1. Study site and sampling**

136 Midtre Lovénbreen is an Arctic polythermal valley glacier on the south side of Kongsfjorden, Western
137 Svalbard (latitude 78°55'N, longitude 12°10'E) (Fig. 1). The Midtre Lovénbreen catchment is roughly 5
138 km East of Ny-Ålesund, where several long-term monitoring programs have provided a wealth of
139 contextual information. Midtre Lovénbreen has experienced negative mass balance throughout much
140 of the 20th century. Since the end of the Little Ice Age (maximum in Svalbard in the 1900s) the de-
141 glaciated surface area of the Midtre Lovénbreen catchment has increased considerably in response to
142 warming mean annual temperatures. This continues to the present day. Between 1966 and 1990 ~ 2.3
143 km² of land was exposed (Fleming et al., 1997; Moreau et al., 2008). We used a chronosequence
144 approach to determine ages for soils based on satellite imagery (Landsat TM 7) and previously
145 determined soil ages by aerial photography and carbon-14 dating techniques in Hodgkinson et al. (2003).
146 Soil samples were collected along a transect perpendicular to the glacier snout, representing soil ages
147 of 0, 3, 5, 29, 50, and 113 years (Fig. 1) during the field season (18 July to 29 August 2013). At each of
148 the 6 sites along the chronosequence, 10 meter traverses roughly parallel to the glacier snout were
149 established and at each site 3 soil plots were sampled (using ethanol sterilized sampling equipment).
150 After removing the > 2 cm rock pieces at each site, about 100 grams of soil was collected from the top
151 15 cm and immediately placed into sterile high-density polyethylene bags (Whirl-Pak (Lactun,
152 Australia)) and into a cool box partially filled with cool packs and dry ice. Samples were immediately
153 frozen and stored at -20°C on return to the UK Arctic Research station in Ny-Ålesund (no longer than 5
154 hours after collection). Samples were transported frozen on dry ice to the laboratories in the Universities
155 of Bristol and Leeds (UK).

156

157 **2.2. Laboratory analyses**

158 For bacterial abundance, samples were thawed and aliquots (100 mg) were immediately transferred
159 into sterile 1.5 mL micro-centrifuge (Eppendorf) tubes, where they were diluted with 900 µL of Milli-Q
160 water (0.2 µm filtered) and immediately fixed in 100 µL glutaraldehyde (0.2 µm filtered, 2.5% final

161 concentration). Samples were then vortexed for 10 seconds and sonicated for 1 minute at 30°C to
162 facilitate cell detachment from soil particles. Then 10 µL fluorochrome DAPI (4', 6-diamidino-2
163 phenylindole) was added to half of the samples, tubes were vortexed briefly (3 seconds) and incubated
164 in the dark for 10 minutes, to be counted under UV light. The other half of each sample remained
165 untreated, for counting under auto-fluorescent light for photosynthetic pigmentation. Samples were
166 vortexed for 10 seconds and let stand for a further 30 seconds to ensure a well-mixed solution, prior to
167 filtering 100 µL of the mixed liquid sample onto black Millipore Isopore membrane filters (0.2 µm pore
168 size, 25 mm diameter), rinsed with a further 250 µL of Milli-Q water (0.2 µm filtered). Bacterial cells were
169 then counted using an Olympus BX41 microscope at 1000 times magnification. The filtering apparatus
170 was washed out with Milli-Q water between each filtration, and negative control samples, prepared
171 using Milli-Q water, were included into each series. A negative control was a sample with no visible
172 stained or auto-fluorescing cells. Thirty random grids (each 10⁴ µm²) were counted per sample. Cell
173 morphologies were measured and cell volume was estimated and converted to carbon content
174 according to Bratbak and Dundas (1984) (see Supplementary Information). Separate aliquots of soil
175 from each site were weighed after thawing and then dried at 105°C to obtain an estimate of soil moisture
176 content.

177

178 Environmental DNA was isolated from at least 3 replicates for each soil age using MoBio [PowerMax®](#)
179 [Soil DNA Isolation Kit](#) ~~PowerSoil® DNA Isolation Kit~~ and by following the instruction manual. 5 to 10 g
180 of soil was used per sample to isolate DNA. [Following extraction, DNA was diluted to equimolar](#)
181 [concentrations, so that all samples contained 7.0 ng of DNA, prior to amplification.](#) The isolated ~~16S~~
182 ~~genomic~~ DNA was amplified with bacterial primers 515f (5'-GTGYCAGCMGCCGCGGTAA-3') and
183 926r (5'-CCGYCAATTYMTTTRAGTTT-3') (Caporaso et al., 2012), creating a single amplicon of ~400
184 bp. The reaction was carried out in 50 µL volumes containing 0.3 mg mL⁻¹ Bovine Serum Albumin, 250
185 µM dNTPs, 0.5 µM of each primer, 0.02 U Phusion High-Fidelity DNA Polymerase (Finnzymes OY,
186 Espoo, Finland) and 5x Phusion HF Buffer containing 1.5 mM MgCl₂. The following PCR conditions
187 were used: initial denaturation at 95°C for 5 minutes, followed by 25 cycles consisting of denaturation
188 (95°C for 40 seconds), annealing (55°C for 2 minutes) and extension (72°C for 1 minute) and a final
189 extension step at 72°C for 7 minutes. ~~S~~ [Following amplification, all amplicons were normalized to the](#)
190 [same concentration \(9.0 ng\) before sequencing.](#) Samples were sequenced using the Ion Torrent
191 platform (using Ion 318v2 chip) at Bristol Genomics facility at the University of Bristol. Samples were
192 barcoded in the PCR stage and demultiplexed in QIIME using split_libraries.py code (Caporaso et al.,
193 2010). A non-barcoded library was prepared from the amplicon pool using Life technologies Short
194 Amplicon Prep Ion Plus Fragment Library Kit. The template and sequencing kits used were: Ion PGM
195 Template OT2 400 Kit and Ion PGM Sequencing 400 kit. The sequencing yielded 4.38 million reads.
196 The 16S sequences were further processed using MOTHUR (v. 1.35) and QIIME pipelines (Schloss et
197 al., 2009; Caporaso et al., 2010). Initially, low quality or too long and too short sequences were removed
198 in MOTHUR. Chimeric sequences were identified and removed using UCHIME (Edgar et al., 2011).
199 QIIME was used to cluster reads into operational taxonomical units (OTUs) using the
200 pick_closed_reference_otus.py command. [The final OTU table contained between 2329-43269 reads](#)

201 [for each sample. The varying sequence coverage among samples was adjusted by normalizing the](#)
202 [OTU matrix to the same total abundance of sequences for each sample \(2329\) using the command](#)
203 [normalize_table.py in QIIME](#). Sequences were clustered into OTUs based on at least 97% sequence
204 similarity, and assigned taxonomical identification against Greengenes bacterial database (McDonald
205 et al., 2012). The result was a biom format file containing the taxonomic information for each OTU as
206 well as OTU frequency per sample. [Sequence data is available on NCBI under project ID](#)
207 [PRJNA341831, and individual accession numbers are provided in the Supplementary Information.](#)
208

209 The carbon contents in the year 0 soils were analysed with a Carlo-Erba elemental analyser (NC2500)
210 at the German Research Center for Geosciences, Potsdam, Germany. The soils were oven dried at
211 40°C for 48 hours, sieved to <7 mm and crushed using a TEMA disk mill to achieve size fractions of <
212 20 µm. Total organic carbon (TOC) was analysed after reacting the powders with a 10% HCl solution
213 for 12 hours to remove inorganic carbonates.
214

215 **2.3. Determination of maximum growth rates**

216 The microbial activity was determined in 113 year old soil samples after they were thawed (in the dark
217 at 5°C to mimic typical field temperature) for 168 hours. This age was chosen because these soil
218 samples were assumed to be the ones with the highest microbial biomass and activity and thus the
219 most practical for all laboratory measurements. In order to mitigate the effect of variability derived from
220 differences in soil properties between soil ages (that will later be predicted by the model), laboratory
221 experiments were conducted on a single soil age, with replicate incubations to assess the possible
222 variability in rates (and thus parameter values) that can be attributed to experimental procedures and
223 measurement techniques.
224

225 Aliquots of the soils were divided into petri dishes (25 g of soil (wet weight) into each petri dish) for
226 subsequent treatments. In order to alleviate nutrient limitations and measure maximum growth rates,
227 four different nutrient conditions were simulated: (1) no addition of nutrients, (2) low (0.03 mg C g⁻¹,
228 0.008 mg N g⁻¹, 0.02 mg P g⁻¹), (3) medium (0.8 mg C g⁻¹, 0.015 mg N g⁻¹, 0.1 mg P g⁻¹) and (4) high
229 additions (2.4 mg C g⁻¹, 0.024 mg N g⁻¹, 0.3 mg P g⁻¹). The ranges and concentrations were informed
230 by similar experiments in recently exposed proglacial soils at the Damma Glacier, Switzerland
231 (Goransson et al., 2011). Nutrients (C₆H₁₂O₆ for C, NH₄NO₃ for N and KH₂PO₄ for P) (Sigma, quality
232 ≥99.0%) were dissolved in 2 mL Milli-Q water (0.2 µm filtered), and mixed into the soils using an ethanol-
233 sterilized spatula. Samples were incubated in the dark for a further 72 hours with the lids on at 25°C,
234 the reference temperature (T_{ref}) at which all rates are defined in SHIMMER prior to adjustment with the
235 temperature dependency expression (using Q_{10}) (Bradley et al., 2015). In order to derive a value for
236 I_{maxH} , we were obligated to perform growth incubations at T_{ref} (25°C) despite this being a more typical
237 soil temperature of Alpine soils rather than High-Arctic soils (see Fig. S3 (c)). However, we are confident
238 that by deriving a Q_{10} value based on incubations of the same soils encapsulating typical (5°C) to high
239 (25°C) soil temperatures, we can numerically derive appropriate actual growth rates from the maximum
240 growth rate (at T_{ref}). We are confident that the major outcomes and conclusions of this study are not

241 affected by high incubation temperatures since measured growth rates at high temperatures are
242 appropriately scaled using the Q_{10} formulation as measured experimentally. Throughout the whole
243 incubation time, at 24 hour intervals, additional 2 mL aliquots of Milli-Q water (0.2 μm filtered) were
244 added to maintain approximate soil moisture conditions in each sample.

245

246 In these samples bacterial production was estimated by the incorporation of ^3H -leucine using the
247 microcentrifuge method detailed in Kirchman (2001). After the initial 72 hour incubation period
248 quadruplicate sample aliquots from the petri dish incubations and two trichloroacetic acid (TCA) killed
249 control samples were incubated for 3 hours at T_{ref} (25°C) for every nutrient treatment. Approximately
250 50 mg of soil was transferred to sterile micro-centrifuge tubes (2.0 mL, Fischer Scientific). Milli-Q (0.2
251 μm pre-filtered) water and ^3H -leucine was added to a final concentration of 100 nM (optimum leucine
252 concentration was pre-determined by a saturation experiment, Fig. S1, Supplementary Information).
253 The incubation was terminated by the addition of TCA to each tube. Tubes were then centrifuged at
254 15,000 g for 15 minutes, the supernatant was aspirated with a sterile pipette and removed, and 1 ml
255 ice-cold 5% TCA was added to each tube. Tubes were then centrifuged again at 15,000g for 5 minutes,
256 before again aspirating and removing the supernatant. 1mL ice-cold 80% ethanol was added and tubes
257 were centrifuged at 15,000 g for 5 minutes, before the supernatant was aspirated and removed again
258 and tubes were left to air dry for 12 hours. Finally, 1 mL of scintillation cocktail was added, samples
259 were vortexed, and then counted by liquid scintillation (Perkin Elmer Liquid Scintillation Analyzer, Tri-
260 Carb 2810 TR). Radioisotope activity of TCA-killed control samples was always less than 1.1% of the
261 measured activity in live samples. There was a positive correlation between the amount of sediment
262 added to the tubes and background counts representing disintegrations per minute (DPM). Counts were
263 individually normalized by the amount of sediments (corrected for dry weight) used in each sample to
264 discount for background DPM. Leucine incorporation rates were converted into bacterial carbon
265 production following the methodology of Simon and Azam (1989). Bacterial abundance was estimated
266 from each treatment after the 72 hour incubation period by microscopy. Five samples from each petri
267 dish were counted for each nutrient treatment with negative controls yielding no detectable cells. One-
268 way ANOVA (with post-hoc Tukey HSD) statistical tests were used for evaluations of the variability from
269 the multiple treatments.

270

271 **2.4. Temperature response**

272 Microbial community respiration was determined by measuring CO_2 gas exchange rates in airtight
273 incubation vials. Soil samples from the 113 year old site were defrosted and divided (25 g wet weight)
274 in petri dishes as above, and 2 mL of Milli-Q water (0.2 μm filtered) was added (to maintain consistency
275 of soil moisture with determination of bacterial production above). Samples were incubated at 5°C (T_1)
276 and 25°C (T_2) in the dark for a further 72 hours. 2mL of 0.2 μm pre-filtered Milli-Q water was added to
277 the T_1 sample (3 mL for T_2) at 24, 48 and 72 hours to maintain approximate soil moisture content. Two
278 separate killed control tests (one furnaceed at 450°C for 4 hours, and one autoclaved (3 cycles at 121°C))
279 were incubated at T_1 and T_2 . Quintuple live and killed samples (roughly 1 g) were transferred into
280 cleaned 20 mL glass vials (rinsed in 2% Decon, submersed in 10% HCl for 24 hours, rinsed 3 times

281 with Milli-Q water and furnace at 450°C for 4 hours). These were sealed (9°C, atmospheric pressure,
282 ambient CO₂ of 405 ppm) with pre-sterilized Bellco butyl stoppers (pre-sterilized by boiling for 4 hours
283 in 1M sodium hydroxide) and crimped shut with aluminium caps. Sealed vials were then incubated at
284 T₁ and T₂ for 24 hours in darkness. After 24 hours, the headspace gas was removed with a gas-tight
285 syringe and immediately analysed on an EGM4 gas analyser (PP Systems, calibrated using gas
286 standards matching the expected range, precision 1.9%, 2*SE). Empty pre-sterilized vials were also
287 incubated and analysed. Following gas analysis, vials were opened and dried to a constant weight at
288 105°C to estimate moisture content and thus dry soil weight of these aliquots. Headspace CO₂ change
289 (ppm) was converted to microbial respiration using the ideal gas law ($n=PV/RT$), assuming negligible
290 changes in soil pore water pH (and therefore CO₂ solubility) during the incubation. CO₂ headspace
291 changes resulting from killed controls and blanks were < 70% of the changes resulting from the
292 incubations at T₁, and <7% of the changes observed at T₂. One-way ANOVA (with post-hoc Tukey
293 HSD) statistical tests were used for comparison of multiple treatments. No significant differences in CO₂
294 headspace change between killed controls at T₁ and T₂ were detected (P=0.95).

295

296 **2.5. Microbial Model: SHIMMER**

297 SHIMMER (Bradley et al., 2015) mechanistically describes and predicts transformations in carbon,
298 nitrogen and phosphorus through aggregated components of the microbial community as a system of
299 interlinked ordinary differential equations. The model contains pools of microbial biomass, organic
300 matter and both dissolved inorganic and organic nitrogen and phosphorus (Table 1). It categorizes
301 microbes into autotrophs (A₁₋₃) and heterotrophs (H₁₋₃), and further subdivides these based on 3 specific
302 functional traits. Microbes derived from underneath the glacier (referred to as “glacial microbes”) are
303 termed A₁ and H₁. A₁ are chemolithoautotrophic, obtaining energy from the oxidation and reduction of
304 inorganic compounds and carbon from the fixation of carbon dioxide. In contrast, H₁ rely on the
305 breakdown of organic molecules for energy to support growth. A₂ and H₂ represent autotrophic and
306 heterotrophic microbes commonly found in glacier forefield soils with no “special” characteristics, and
307 will be referred to as “soil microbes”. A₃ and H₃ are autotrophs and heterotrophs that are able to fix
308 atmospheric N₂ gas as a source of nitrogen in cases when dissolved inorganic nitrogen (DIN) stocks
309 become limiting. Available organic substrate is assumed to be derived naturally from dead organic
310 matter and allochthonous inputs. Labile compounds are immediately available fresh and highly reactive
311 material, rapidly turned over by the microorganisms (S₁, ON₁, OP₁). Refractory compounds are less
312 bioavailable and represents the bulk of substrate present in the non-living organic component of soil
313 (S₂, ON₂, OP₂). A conceptual diagram showing the components and transfers of SHIMMER is presented
314 in the Supplementary Information (Fig. S2).

315

316 Microbial biomass responds dynamically to changing substrate and nutrient availability (expressed as
317 Monod-kinetics), as well as changing environmental conditions (such as temperature and light). A Q₁₀
318 temperature response function (T_f) is affixed to all metabolic processes including growth rates and death
319 rates (Bradley et al., 2015), thus effectively slowing down or speeding up all life processes as
320 temperature changes (Soetaert and Herman, 2009; Yoshitake et al., 2010; Schipper et al., 2014). Light

321 limitation is expressed as Monod kinetics. The following external forcings drive and regulate the
322 system's dynamics:

- 323 • Photosynthetically-active radiation (PAR) (wavelength of approximately 400 to 700 nm) ($W m^{-2}$).
324
- 325 • Snow depth (m).
- 326 • Soil temperature ($^{\circ}C$).
- 327 • Allochthonous inputs ($\mu g g^{-1} day^{-1}$).

328

329 The model is 0-D and represents the soil as a homogeneous mix. Thus, light, temperature, nutrients,
330 organic compounds and microbial biomass are assumed to be evenly distributed.

331

332 Soil temperature (at 1 cm depth) for the entire of 2013 is provided by Alfred Wegener Institute for Polar
333 and Marine Research (AWI) from the permafrost observatory near Ny-Ålesund, Svalbard. Similarly,
334 PAR for 2013 are measured at the AWI surface radiation station near Ny-Ålesund, Svalbard. Averaged
335 daily snow depth for 2009 to 2013 is provided by the Norwegian Meteorological Institute (eKlima).
336 Allochthonous nutrient fluxes (inputs and leaching) are estimated based on an evaluation of nutrient
337 budgets of the Midtre Lovénbreen catchment (Hodson et al., 2005) in which budgets for nutrient
338 deposition rates and runoff concentrations are measured over two full summer-winter seasons and
339 residual retention rates (excess of inputs) or depletion rates (excess of outputs) are inferred. The
340 bioavailability of allochthonous material is assumed to be the same as initial material and microbial
341 necromass.

342

343 Initial conditions were informed by analysis of 0-years-of-exposure soil collected adjacent to the ice
344 snout, and initial values for all state variables are presented in Table 1. Initial microbial biomass was
345 estimated by microscopy as described above. Initial community structure was derived by 16S analysis
346 of year-0 soils. An initial value for carbon substrate ($S_1 + S_2$) was estimated based on the average TOC
347 content of year-0 soil. Bioavailability of model TOC was assumed to be 30% labile (S_1) and 70%
348 refractory (S_2) (for consistency with Bradley et al. (2015)). Organic nitrogen (ON) and organic
349 phosphorus (OP) were assumed to be stoichiometrically linked by the measured C:N:P ratio from the
350 Damma Glacier forefield (from which the model was initially developed and tested (Bradley et al.,
351 2015)). An initial value for DIN was taken from a previous evaluation of Svalbard tundra nitrogen
352 dynamics, whereby the lowest value is taken to represent the soil of least development, according to
353 traditional understanding of glacier forefields (Alves et al., 2013; Bradley et al., 2014). An initial value
354 for dissolved inorganic phosphorous (DIP) was established stoichiometrically from previous model
355 development and testing.

356

357 Model implementation and set-up is described in more detail in the Supplementary Information.

358

359 **2.6. Model parameters**

360 Maximum heterotrophic growth rate I_{maxH} (day^{-1}) was estimated by scaling the measured rate of bacterial
361 production ($\mu\text{g C g}^{-1} \text{ day}^{-1}$) (converted to dry weight) with total heterotrophic biomass ($\mu\text{g C g}^{-1}$). Nutrient
362 addition alleviates growth limitations as defined in SHIMMER (Bradley et al., 2015); thus bacterial
363 communities can be assumed to be growing at I_{maxH} under experimental conditions.

364

365 Y_H represents heterotrophic BGE, and was estimated according to the equation:

366

$$367 \quad Y_H = \frac{BP}{BP + BR} \quad (1)$$

368
369 Where BP is and BR are measured bacterial production and measured bacterial respiration ($\mu\text{g C g}^{-1}$
370 day^{-1}) respectively, at 25°C with no nutrients added.

371

372 The temperature response (Q_{10}) value was estimated as:

373

$$374 \quad Q_{10} = \left(\frac{R_2}{R_1}\right)^{\left(\frac{10}{T_2 - T_1}\right)} \quad (2)$$

375
376 Where R_1 and R_2 represent the measured respiration rate ($\mu\text{g C g}^{-1} \text{ day}^{-1}$) at temperatures T_1 and T_2
377 (5°C and 25°C).

378

379 Laboratory-defined parameters (i.e. growth rate, temperature sensitivity and BGE) were assumed to be
380 the same for all microbial groups. A complete list of parameters and values is presented in Table S3
381 (Supplementary Information).

382

383 3. Results

384 3.1. Laboratory results and model parameters

385 Bacterial production in untreated soil was estimated at $0.76 \mu\text{g C g}^{-1} \text{ day}^{-1}$ ($\text{SD}=0.12$), and across all
386 nutrient treatments ranged from 0.560 to $2.196 \mu\text{g C g}^{-1} \text{ day}^{-1}$. Nutrient addition led to increased
387 measured production (low = $0.69 \mu\text{g C g}^{-1} \text{ day}^{-1}$ ($\text{SD}=0.12$), medium = $1.09 \mu\text{g C g}^{-1} \text{ day}^{-1}$ ($\text{SD}=0.53$),
388 high = $1.52 \mu\text{g C g}^{-1} \text{ day}^{-1}$ ($\text{SD}=0.63$)), however variability between replicates was also high and
389 production rates from each nutrient treatment were not significantly different from untreated soil
390 ($P_{\text{low}}=0.99$, $P_{\text{medium}}=0.70$, $P_{\text{high}}=0.10$). The increased bacterial production was cross-correlated with
391 quadruplicate measurements of biomass from each treatment, and resulting growth rate coefficients
392 (I_{maxH}) for all treatments were within a narrow range (0.359 to 0.550 day^{-1}) and there was no statistically
393 significant difference in growth rates between each nutrient treatment (Fig. 2b) ($P_{\text{low-medium}}=0.55$, $P_{\text{medium-}}$
394 $\text{high}}=0.49$, $P_{\text{none-high}}=0.10$). The maximum measured growth rate for a single nutrient treatment, thus
395 equating to the parameter I_{maxH} , was 0.55 day^{-1} . The 95% confidence range for I_{maxH} is 0.50 to 0.60 day^{-1} .
396 This value is, to our knowledge, is the first measured rate of bacterial growth from High-Arctic soils,
397 and falls within the lower end of the plausible range established in Bradley et al. (2015) ($0.24 - 4.80$
398 day^{-1}) (Fig. 3a) for soil microbes from a range of laboratory and modelling studies (Frey et al., 2010;

399 Ingwersen et al., 2008; Knapp et al., 1983; Zelenev et al., 2000; Stapleton et al., 2005; Darrah, 1991;
400 Blagodatsky et al., 1998; Vandewerf and Verstraete, 1987; Foereid and Yearsley, 2004; Toal et al.,
401 2000; Scott et al., 1995). For respiration, significantly higher CO₂ headspace concentration were
402 detected in the live incubations at 25°C relative to killed controls ($P < 0.05$). Average respiration rate at
403 5°C was 1.61 $\mu\text{g C g}^{-1} \text{ day}^{-1}$ and there was a significant increase in soil respiration at 25°C (12.83 $\mu\text{g C}$
404 $\text{g}^{-1} \text{ day}^{-1}$) (Fig. 2c) ($P < 0.05$). The Q_{10} value for Midtre Lovénbreen forefield soils was thus calculated
405 as 2.90, and a 95% confidence range was established as 2.65 to 3.16. This was at the upper end of the
406 plausible range previously identified in Bradley et al. (2015) (Fig. 3b). Based on measured values of
407 bacterial production and respiration, BGE (Y_H) was 0.06, with a 95% confidence range of 0.05 to 0.07
408 (Fig. 3c). Final calculated values for model parameters are summarized in Table S3 (Supplementary
409 Information).

410

411 The results from microscopy determination of biomass are presented in Table 2. In the freshly exposed
412 soil (year 0) heterotrophic biomass was low (0.059 $\mu\text{g C g}^{-1}$), increased substantially to 0.244 $\mu\text{g C g}^{-1}$
413 in 29 year old soils, and was an order or magnitude higher (2.00 $\mu\text{g C g}^{-1}$) in 113 year old soils.
414 Autotrophic biomass was considerably higher than heterotrophic biomass and increased by roughly an
415 order of magnitude from year 0 (0.171 $\mu\text{g C g}^{-1}$) to year 29 (1.07 $\mu\text{g C g}^{-1}$) and approximately doubled
416 by year 113 (2.58 $\mu\text{g C g}^{-1}$). TOC in freshly exposed soil was approximately 0.793 mg C g^{-1} .

417

418 16S data was categorized into microbial groups (A_{1-3} and H_{1-3}) as defined by the model formulation.
419 Chemolithoautotrophs, such as known iron or sulphur oxidizers (genera *Acidithiobacillus*, *Thiobacillus*,
420 *Gallionella*, *Sulfurimonas*) were assigned into the A_1 group. Phototrophic microorganisms, such as
421 cyanobacteria (*Phormidium*, *Leptolyngbya*) and phototrophic bacteria (*Rhodospirillum rubrum*, *Erythrobacter*,
422 *Halomicronema*) were allocated into group A_2 , while heterocyst forming cyanobacteria from the orders
423 Nostocales and Stigonematales were assigned to group the A_3 (nitrogen-fixing autotrophs). Members
424 of the family Comamonadaceae of the Betaproteobacteria are known glacial dwelling microorganisms
425 (Yde et al., 2010) and were thus included into the group H_1 . General soil heterotrophic microorganisms
426 (mainly members of Alphaproteobacteria, Actinobacteria, Bacteroidetes and Acidobacteria) were
427 assigned into group H_2 (general soil heterotrophs). Lastly, group H_3 consisted of heterotrophic nitrogen
428 fixers, mainly *Azospirillum*, *Bradyrhizobium*, *Devosia*, *Clostridium*, *Frankia* and *Rhizobium*. Pathogens,
429 non-soil microorganisms and organisms with unknown physiological traits were assigned into the
430 "Uncategorized" group. Glacial microbes accounted for 43 to 45 % of reads in year 0 and 5, and declined
431 in older soils (year 50 and 113) to 18 to 22%. The glacial community was predominantly
432 chemolithoautotrophic (A_1). Typical soil bacteria (A_2 and H_2) increased from low abundance (30% and
433 40% in years 0 and 5 respectively) to relatively high abundance (63 to 67% of reads) in years 50 and
434 113. Nitrogen fixing bacteria were prevalent in recently exposed soils (14% in year 0) but low in relative
435 abundance in soils above 5 years of age (4 to 6% in years 5, 50 and 113). In the freshly exposed soil
436 (year 0), the microbial community was relatively evenly distributed between heterotrophs (43%) and
437 autotrophs (44%). In developed soils, the relative abundance of heterotrophs increased (up to 74% of

438 reads in years 50 and 113). Important to note is the fact that between 8 and 21% of the reads across
439 all samples could not be classified.

440

441 **3.2. Model Results**

442 The model predicted an accumulation of autotrophic and heterotrophic biomass over 120 years (Fig.
443 4a and 4b). Biomass and nutrient concentrations were initially extremely low (total biomass < 0.25 μg
444 C g^{-1} , DIN < 4.0 $\mu\text{g N g}^{-1}$, DIP < 3.0 $\mu\text{g P g}^{-1}$), and biological activity in initial soils was also low (Table
445 3). There was an order of magnitude increase in total microbial biomass in years 10 to 60. Nitrogen-
446 fixing autotrophs (A_3) and heterotrophs (H_3), and soil heterotrophs (H_2) experienced rapid growth during
447 this period. Glacial and soil autotrophs (A_{1-2}) and glacial heterotrophs (H_1) remained low. Bacterial
448 production increased by roughly two orders of magnitude (Table 3). Organic carbon (labile and
449 refractory) increased (Fig. 4c), whilst DIN and DIP concentrations increased by approximately an order
450 of magnitude in the first 60 years (Fig. 4d). During the later stages of soil development (years 60 to
451 120), biomass increased rapidly due to the rapid growth of soil organisms (A_2 and H_2), which
452 outcompeted nitrogen-fixers. The model showed a rapid exhaustion of labile organic carbon (years 50
453 to 100), while refractory carbon accumulated slowly. Nutrients (DIN and DIP) accumulated at a relatively
454 constant rate. Microbial activity, including bacterial production, nitrogen fixation and DIN assimilation,
455 was high relative to early stages (Table 3).

456

457 A carbon budget of fluxes through the substrate pool is presented in Fig. 5. Daily fluxes are presented
458 in panels (a) for year 5, (b) for year 50 and (c) for year 113, and annual fluxes up to year 120 are
459 presented in (d). In recently exposed soils (5 years), allochthonous inputs were the only noticeable
460 carbon flux, outweighing heterotrophic growth and respiration, and the contribution of substrate from
461 necromass and exudates by over two orders of magnitude (Fig. 5a). Thus, the total change in carbon
462 (black line) closely resembled allochthonous input. In the intermediate stages (Fig. 5b), there was
463 substantial depletion from the substrate pool due to heterotrophic activity. Heterotrophic growth (red
464 line) was low despite high substrate consumption and respiration (dark blue line). In the late stages of
465 soil development, the flux of microbial necromass was a significant contributor to the organic substrate
466 pools (Fig. 5c). Carbon fluxes in mid to late stages of soil development were highly seasonal (Fig. 5b
467 and 5c). Biotic fluxes (e.g. respiration) were up to six times higher during the summer (July to
468 September) compared to the winter (November to April), however a base rate of heterotrophic
469 respiration and turnover of microbial biomass was sustained over winter. Figure 4d shows that the
470 contribution of microbial necromass rose steadily throughout the simulation (light blue line), however
471 was not sufficient to compensate the uptake of carbon substrate, thus leading to overall depletion
472 between years 50 to 110 (black line). The contribution of exudates (purple line) to substrate was minimal
473 at all soil ages.

474

475 **4. Discussion**

476 **4.1. Determination of parameters and model predictions**

477 Figure 6 illustrates the influence of the site-specific, laboratory-derived parameters on microbial
478 biomass predictions. It compares the range of predicted microbial biomass based on laboratory-
479 determined parameters (yellow) to the entire plausible parameter range (red; Bradley et al. (2015)).
480 Predicted biomass with the average laboratory-derived value is indicated by the black line. For I_{max} ,
481 predicted biomass with laboratory-derived parameters (yellow shading) was towards the lower end of
482 the plausible range (Fig. 6a) because refined growth rates were significantly lower than the maximum
483 values explored previously. This was mostly due to a significant reduction in autotrophic biomass (A_{1-}
484 $_3$). With high growth rates, there was a sharp early increase in biomass (years 10 to 20) followed by
485 slower growth phase (years 20 to 120). Model results with laboratory-derived growth rates showed that
486 the exponential growth phase occurred later (years 40 to 80) and was more prolonged, but total biomass
487 was considerably lower. There was a substantial reduction in the plausible range in predicted microbial
488 biomass.

489

490 There was a substantial reduction in the plausible range in predicted microbial biomass (Fig. 6b) from
491 the measured temperature sensitivity (Q_{10}) (yellow) compared to the previous range (red). Soil microbial
492 communities in Polar regions must contend with extremely harsh environmental conditions such as cold
493 temperatures, frequent freeze-thaw cycles, low water availability, low nutrient availability, high exposure
494 to ultraviolet radiation in the summer, and prolonged periods of darkness in winter. These factors
495 profoundly impact their metabolism and survival strategies and ultimately shape the structure of the
496 microbial community (Cary et al., 2010). High Q_{10} values, as derived here, are typical of cold
497 environments and cold adapted organisms and this has been associated with the survival of biomass
498 under prolonged periods of harsh environmental conditions (Schipper et al., 2014). An investigation into
499 the metabolism of microbial communities in biological soils crusts in recently exposed soils from the
500 Austre Broggerbreen Glacier, approximately 6 km from the Midtre Lovénbreen catchment, also derived
501 a high Q_{10} (3.1) (Yoshitake et al., 2010). The Midtre Lovénbreen catchment, in Svalbard, experiences
502 a relatively extreme Arctic climate. The high Q_{10} ultimately lowers the overall rate of biomass
503 accumulation in ultra-oligotrophic soils and a baseline population is maintained.

504

505 The low measured BGE (0.06) suggested that a high proportion (94%) of substrate consumed by
506 heterotrophs is remineralized (degrading organic substrate into DIC (CO_2), DIN and DIP), with very little
507 being incorporated into biomass (6%). Low BGE encouraged the liberation and release of nutrients to
508 the soil and thus the overall growth response of the total microbial biomass was more rapid due to
509 higher soil nutrient concentrations (Fig. 6c). However, due to the low BGE, there was a high rate of
510 substrate degradation, and as such, labile substrate was rapidly depleted when heterotrophic biomass
511 was high (Fig. 4c). Heterotrophic growth requires that a substantial amount of substrate is degraded –
512 thus, although autotrophic production outweighed heterotrophic production at all stages of development
513 (Fig. 4e), the soil was predicted by the model to be a net source of CO_2 to the atmosphere over the first
514 120 years of exposure (Fig. 4f). Heterotrophic growth and respiration (and thus net ecosystem
515 production and carbon fluxes) are strongly dependant on the availability of soil organic carbon. Poorly
516 quantified rates of allochthonous organic carbon deposition and its quality may lead to generally high

517 uncertainty in the net ecosystem production due to potentially enhanced heterotrophic growth resulting
518 from higher organic carbon deposition, or lower heterotrophic growth resulting from substrate limitation
519 in low-deposition scenarios. Soil CO₂ efflux is highly sensitive to variable net ecosystem production,
520 thus simulated net ecosystem production estimates must be interpreted cautiously until sufficient field
521 data emerges (e.g. from in situ measurement of soil gas exchange). The calculation of BGE assumes
522 that bacterial respiration is the major contributor to measured CO₂ gas exchange rates from soil
523 microcosms. In reality, all active and living soil organisms are likely to contribute to measured CO₂
524 fluxes, however due to limitations with experimental protocols, it is extremely difficult to determine the
525 relative contribution of various organisms to total respiration. Microscopy analysis showed limited
526 presence of fungi and protozoa suggesting that the biological community of the soil community is mainly
527 bacterial. Nevertheless, by attributing total measured CO₂ fluxes solely to bacteria, BGE may be under-
528 estimated (due to an overestimation of respiration rates attributed to the bacterial community). Thus,
529 we cannot exclude that our low BGE values might be in part an artefact of this experimental limitation.
530 However, although there are very few measurements of BGE in cold glaciated environments, our
531 estimate of BGE is in good agreement with previous studies, which have suggested values ranging
532 between 0.0035 and 0.033 (Anesio et al., 2010; Hodson et al., 2007). Therefore, we are confident that
533 BGE values measured here fall within a realistic range.

534

535 Three assumptions are made in the assignment of measured parameters to SHIMMER as applied to
536 the High-Arctic field site. The first assumption of SHIMMER is that parameter values remain constant
537 throughout the duration of the simulation. Empirical evidence suggests that parameters defined as fixed
538 in SHIMMER (e.g. Q_{10}) may be variable over time, however in SHIMMER, like many numerical
539 modelling formulations, changing environmental (temperature, light) and geochemical (carbon
540 substrate, available nitrogen, available phosphorus) conditions drive subsequent variability in microbial
541 activity via mathematical formulations (e.g. Monod kinetics, see Bradley et al. (2015)) affixed to
542 parameter values. A second assumption is the assignment of measured rates to parameters for all
543 microbial functional groups. Rather than taxonomic based classification, SHIMMER distinguishes and
544 classifies microbial communities based on functional traits. These mathematical formulations assigned
545 to, for example, microbial growth, are different between groups to represent distinct functional traits
546 associated with that group. Whilst actual rates may be different between different organisms, for the
547 level of model complexity and outputs required, a community measurement of those parameters is
548 sufficient, particularly considering that the differences are accounted for in the mathematical formulation
549 of SHIMMER (see Bradley et al. (2015)). Third, maximum microbial growth rate at T_{ref} (25°C, Bradley
550 et al. (2015)) as modelled in SHIMMER is modified by Monod terms that account for nutrient limitation
551 (e.g. Monod terms), as well as a temperature response function (Q_{10}) to estimate actual growth rate at
552 ambient temperature. A major objective of of this study was to improve model performance by
553 constraining previously identified key model parameters (see sensitivity study results in Bradley et al.
554 (2015)) through specifically designed laboratory experiments. We showed this by comparing model
555 simulation results applying measured, site-specific parameter with simulation results using a range of
556 parameter values reported in the literature (Fig. 6).

557

558 **4.2. Microbial biomass dynamics and community structure**

559 Measured microbial biomass in the initial soils of Midtre Lovénbreen ($0.23 \mu\text{g C g}^{-1}$, 0 years) was very
560 low compared to initial soils in other deglaciated forefields of equivalent ages in lower latitudes, for
561 example in the Alps ($4 \mu\text{g C g}^{-1}$) (Bernasconi et al., 2011; Tscherko et al., 2003) and Canada ($6 \mu\text{g C g}^{-1}$)
562 (Insam and Haselwandter, 1989). However, our microbial biomass values are more similar to other
563 recently deglaciated soils in Antarctica (Ecology Glacier - $0.88 \mu\text{g C g}^{-1}$) (Zdanowski et al., 2013). Low
564 biomass is possibly a result of the harsh, ultra-oligotrophic and nutrient limiting environment of the High
565 Arctic and Antarctica, where low temperature and longer winters limit the summer growth phase,
566 especially compared to an Alpine system (Tscherko et al., 2003; Bernasconi et al., 2011).

567

568 The initial microbial community structure in our samples was predominantly autotrophic (74.5%). In the
569 years following exposure, we observed an increase in autotrophs and heterotrophs with soil age (Table
570 2), presumably due to the establishment and growth of stable soil microbial communities (Schulz et al.,
571 2013; Bradley et al., 2014). Both the observations and modelling results suggested that there was no
572 substantial increase in heterotrophic biomass during the initial and early-intermediate stages of soil
573 development (years 0 to 40), which was then followed by a growth phase whereby biomass increased
574 by roughly an order of magnitude. Overall, the model and the microscopy data were in good agreement
575 accounting for the limitations in both techniques, spatial heterogeneity, and the oscillations in biomass
576 arising from seasonality (Fig. 7). SHIMMER predicted that low initial microbial populations have the
577 potential to considerably increase in population density during several decades of soil development.
578 This data thus supports the hypothesis that the observed increase in microbial biomass with soil age is
579 a consequence of *in situ* growth and activity. The pattern of microbial abundance observed in the Midtre
580 Lovénbreen forefield broadly resembles that of other glacier forefields worldwide (see Bradley et al.
581 (2014)). For example, data from the Rootmoos Ferner (Austria) (Insam and Haselwandter, 1989),
582 Athabasca (Canada) (Insam and Haselwandter, 1989), Damma (Switzerland) (Bernasconi et al., 2011;
583 Schulz et al., 2013) and Puca (Peru) (Schmidt et al., 2008) glacier forefields find increased microbial
584 biomass and activity over decades to centuries of soil development following exposure.

585

586 The genomic data indicated that glacial microbes (such as members of the family Comamonadaceae.)
587 are dominant in recently exposed soils, in agreement with model results (Fig. 8). The community
588 structure in year 5 was heavily dominated by chemolithoautotrophs (A_1) (including taxa *Thiobacillus*,
589 *Rhodoplanes*, *Acidithiobacillus*, *Nitrospira*, *Sulfurimonas* and others), which reflected findings from
590 previous studies whereby chemolithoautotrophic bacteria contribute to the oxidation of FeS_2 in
591 proglacial moraines in Midtre Lovénbreen (Borin et al., 2010; Mapelli et al., 2011). These processes are
592 also commonly described in other subglacial habitats (Boyd et al., 2014; Hamilton et al., 2013). Based
593 on 16S data, the glacial community declined in relative abundance with soil age. This finding was also
594 reflected in the model in years 50 and 113. As the age of the soil progressed, there was typically greater
595 abundance of microbes representing typical soil bacteria (groups A_2 and H_2 including taxa *Geobacter*,
596 *Micrococcus*, *Actinoplanes*, *Sphingomonas*, *Pedobacter* and *Devosia*, *Frankia*, *Rhizobium*) in the 16S

597 data and the model, thus the relative abundance of glacial microbes decreased. Relative abundance of
598 microbial communities across the chronosequence is plotted at the phylum and genus level in the
599 Supplementary Information (Fig. S4 and S5). The overall trends show the relative increase in the
600 proportion of Acidobacteria with the soil age. They contain typical soil bacteria and are thus often used
601 as markers of soil formation and soil development. They are usually associated with plant covered older
602 soils with lower pH as they specialize in degradation of plant recalcitrant organic compounds. The
603 younger soils, on the other hand contained relatively higher proportion of sequences of Proteobacteria
604 (particularly Betaproteobacteria), Bacteroidetes and Cyanobacteria, i.e. groups often associated with
605 supra or subglacial habitats.

606

607 Microscopic analyses indicated low total biomass in recently exposed soils (up to $1.7 \mu\text{g C g}^{-1}$ in soil
608 exposed for 50 years) that was comprised predominantly of autotrophic bacteria. Model simulations
609 agreed well with microscopy derived data. Overall, the 16S data, when categorised into functional
610 groups as defined by the model, agreed well with the microscopy and model output in the very early
611 stages of soil development. However, in later stages of soil development (50 years and older),
612 microscopy and modelling suggested a continuation of predominantly autotrophic soil microbial
613 communities whereas 16S sequence data notably indicated a predominantly heterotrophic community.
614 With extremely low biomass, cell counts derived from microscopy, as well as representation of relative
615 abundance by 16S extraction and amplification, can be largely skewed by relatively small changes in
616 the soil microbial community. Furthermore, the comparative difficulty to lyse autotrophic bacteria (such
617 as some groups of cyanobacteria) from an environmental sample compared to heterotrophic bacteria,
618 and thus successfully amplify the 16S gene during the PCR process, may skew 16S sequence data in
619 favour of heterotrophic sequence reads. Incomplete sample depth (shown by rarefaction curves, Fig
620 S6), the differential extractability of DNA from different organisms, and variation in rDNA copy number
621 adds potential for error to the presented 16S data, and thus absolute numbers should be treated with
622 caution. Additionally, SHIMMER is an ambitious model in that it attempts to simulate, predict and
623 constrain multiple functional types of bacteria species in a numerical framework. Numerical models
624 containing multiple species or multiple microbial functional groups are often extremely challenging to
625 constrain (Servedio et al., 2014; Hellweger and Bucci, 2009; Jessup et al., 2004; Larsen et al., 2012),
626 and as such, the majority of microbial soil models often only resolve one or two living biomass pool that
627 represents the bulk activity and function of the entire community (see e.g. Manzoni et al. (2004),
628 Manzoni and Porporato (2007), Blagodatsky and Richter (1998), Ingwersen et al. (2008), Wang et al.
629 (2014) and others). Our rationale for resolving six distinct functional groups was to quantitatively assess,
630 using modelling, the relative importance and role of each functional group at different stages of soil
631 development. Regardless of discrepancies in older soils (over 50 years since exposure), both the 16S
632 and microscopy data indicated that there was a mixed community of autotrophs and heterotrophs in
633 soils of all ages, which was supported by modelling, since no functional groups were extirpated over
634 simulations representing 120 years of soil development. Thus, SHIMMER is able to capture the diversity
635 of the samples over 120 years of soil development, but the detailed community composition requires
636 further investigation.

637

638 Nitrogen-fixing bacteria such as *Nostoc*, *Rivularia*, *Pseudanabaena* and *Rhodobacter* were prevalent
639 in recently exposed soils but declined in relative abundance with soil age. By fixing N₂ instead of
640 assimilating DIN, the model predicted that nitrogen-fixers were able to grow rapidly in the early stages
641 relative to other organisms (Fig. 4a, 4b). The model prediction supports findings by previous studies
642 demonstrating the importance of nitrogen fixation in Alpine (Duc et al., 2009; Schmidt et al., 2008) and
643 Antarctic (Strauss et al., 2012) glacier forefields and other High-Arctic (Svalbard, Greenland) glacial
644 ecosystems (Telling et al., 2011; Telling et al., 2012). However, there was poor agreement on the
645 relative abundance of nitrogen-fixers between the model and the 16S data in the later stages of soil
646 development (years 50 to 120), particularly between autotrophs and heterotrophs. The model over-
647 predicted the relative abundance of nitrogen-fixing organisms (Fig. 8). The majority of the biomass of
648 the autotrophic nitrogen-fixers was composed of sequences belonging to the cyanobacterium from the
649 genus *Nostoc*. *Nostoc* forms macroscopically visible colonies that grow on the surface of the soils. Its
650 distribution in the Arctic soils is thus extremely patchy and therefore, part of the discrepancy between
651 the 16S data and the model regarding the relative distribution of the A₃ group in the older soils could be
652 due to under-sampling of the *Nostoc* colonies as a consequence of a random sampling approach.
653 Furthermore, allochthonous inputs of nitrogen to the Arctic (e.g. aerial deposition (Geng et al., 2014))
654 strongly affect the productivity of microbial ecosystems and the requirement of nitrogen fixation for
655 microbes (Bjorkman et al., 2013; Kuhnelt et al., 2013; Kuhnelt et al., 2011; Hodson et al., 2010; Telling
656 et al., 2012; Galloway et al., 2008). Thus, uncertainty in the allochthonous availability of nitrogen
657 strongly affects nitrogen fixation rates. In attempting to replicate a qualitative understanding of the
658 nitrogen cycle in a quantitative mathematical modelling framework, the predicted importance of
659 nitrogen-fixing organisms may be over-estimated. The poor agreement in the relative abundance of
660 nitrogen-fixers between the model and the 16S data indicates an incomplete understanding of
661 allochthonous versus autochthonous nutrient availability. Allochthonous nutrient availability is a known
662 source of uncertainty (Bradley et al., 2014; Schulz et al., 2013; Schmidt et al., 2008), and addressing
663 this concern is the subject of future work.

664

665 16S data is an exciting resource of information that is rarely (or never) used to test numerical process-
666 based biogeochemical models. However, the environment (difficulty to extract DNA), the presentation
667 (percentages of low concentration and thus easy to shift relative abundance), the potentially high
668 proportion of dead or dormant cells (which may be present in sequence data but are not necessarily
669 metabolically active), [the differential extractability of DNA from different organisms and variation in](#)
670 [rDNA copy number](#), and uncertainties in model formulation make comparisons challenging. In making
671 this first attempt at comparison of model output to 16S data, we hope to spark discussion and further
672 development of approaches that have similar objectives in order to improve future model
673 performance.

674

675 **4.3. Net ecosystem metabolism and carbon budget**

676

677 Allochthonous carbon inputs were the most significant contributor to recently exposed soils (e.g. year
678 5), since the total change in substrate closely followed this flux (Fig. 5). In older soils (year 113), biotic
679 fluxes were substantially higher, and microbial necromass contributed equally as a source of organic
680 substrate compared to allochthonous deposition. In the older soils, heterotrophic growth and respiration
681 caused substantial consumption and thus depletion of available carbon stocks. This evidence thus
682 supports the hypothesis that carbon fluxes in very recently exposed soils are low and are dominated by
683 abiotic processes (i.e. allochthonous deposition), whereas biotic processes (such as microbial growth,
684 respiration and cell death) play a greater role in developed soils with increased microbial abundance
685 and activity. These findings for the Midtre Lovénbreen glacier in the High-Arctic, are similar to what has
686 been observed based on empirical evidence from Alpine settings (at the Damma Glacier, Switzerland
687 (Smittenberg et al., 2012; Guelland et al., 2013)).

688

689 The seasonality of carbon fluxes predicted by the model (Fig. 5b and 5c) related to the high measured
690 Q_{10} values. High seasonal variation in biotic fluxes and rates is typical of cryospheric soil ecosystems
691 (Schostag et al., 2015) including Alpine glacier forefield soils (Lazzaro et al., 2012; Lazzaro et al., 2015).
692 However, microbial activity has been shown to persist during winter under insulating layers of snow and
693 in sub-zero temperatures (Zhang et al., 2014). Modelling also predicted sustained organic substrate
694 degradation, microbial turnover and net heterotrophy during the winter (Fig. 5b and 5c), as documented
695 in other glacier forefield studies from an Alpine setting (Guelland et al., 2013b).

696

697 The low measured BGE has three important consequences. Firstly, low BGE suggests that a large pool
698 of substrate is required to support heterotrophic growth. Low-efficiency heterotrophic growth lead to the
699 rapid depletion of substrate; therefore high allochthonous inputs were required to maintain a sizeable
700 pool. In older soils (years 80 to 120), increased inputs from microbial necromass (blue line, Fig. 5d)
701 sustained substrate supply to heterotrophs. The sources of allochthonous carbon substrate to the
702 glacier forefield include meltwater inputs derived from the supraglacial and subglacial ecosystems
703 (Stibal et al., 2008; Hodson et al., 2005; Mindl et al., 2007), snow algae (which are known to be prolific
704 primary colonizers and producers in High Arctic snow packs (Lutz et al., 2015; Lutz et al., 2014),
705 atmospheric deposition (Kuhnel et al., 2013) and ornithogenic deposition (e.g. faecal matter of birds
706 and animals) (Jakubas et al., 2008; Ziolek and Melke, 2014; Luoto et al., 2015; Michelutti et al., 2009;
707 Michelutti et al., 2011; Moe et al., 2009). Microbial dynamics are moderately sensitive to external
708 allochthonous inputs of substrate (Bradley et al., 2015), and addressing the uncertainty associated with
709 this flux is an important question to address in future research.

710

711 Secondly, low BGE causes a net efflux of CO_2 over the first 120 years of soil development despite high
712 autotrophic production (Fig. 4e and 4f). Recent literature has explored the carbon dynamics of glacier
713 forefield ecosystems, finding highly variable soil respiration rates (Bekku et al., 2004; Schulz et al.,
714 2013; Guelland et al., 2013a). Future studies should focus on quantifying carbon and nutrient
715 transformations and the potential for forefield systems to impact global biogeochemical cycles in
716 response to future climate change (Smittenberg et al., 2012) and in the context of large-scale ice retreat.

717

718 Thirdly, high rates of substrate degradation encouraged by low BGE were responsible for rapid nutrient
719 release. Modelling suggested that microbial growth was strongly inhibited by low nutrient availability in
720 initial soils ($4 \mu\text{g N g}^{-1}$, 2 to $10 \mu\text{g P g}^{-1}$) (Fig. 4d). This is consistent with findings from the Hailuogou
721 Glacier (Gongga Shan, China) and Damma Glacier (Switzerland) (Prietz et al., 2013). Low BGE is
722 predicted by the model to have a very important role in encouraging the release of nutrients from organic
723 material more rapidly, thereby increasing total bacterial production in the intermediate stages of soil
724 development. Increased nutrient availability with increased heterotrophic biomass is consistent with
725 recent observations from glacier forefields (Bekku et al., 2004; Schulz et al., 2013; Schmidt et al., 2008).

726

727 **5. Conclusions**

728 We used laboratory-based mesocosm experiments to measure three key model parameters: maximum
729 microbial growth rate (I_{max}) (by incorporation of ^3H -leucine), BGE (Y) (by measuring respiration rates)
730 and the temperature response (Q_{10}) (by measuring rates at different ambient temperatures).
731 Laboratory-derived parameters were comparable with previous estimations. We refined model
732 predictions constraining site-specific parameters by lab experiments, thus decreasing parameter
733 uncertainty and narrowing the range of model output over nominal environmental conditions. A
734 comparison of model simulations using laboratory-derived parameter values and previously defined
735 parameter values showed that the coupling of high Q_{10} values and low BGE were important factors in
736 controlling biomass accumulation due to promoting survival of biomass during periods of low
737 temperature, and the enhanced recycling of nutrients through organic matter degradation, respectively.
738 Our results demonstrated that *in situ* microbial growth lead to the overall accumulation of microbial
739 biomass in the Midtre Lovénbreen forefield during the first century of soil development following
740 exposure. Furthermore, carbon fluxes increased in older soils due to elevated biotic (microbial) activity.
741 Microbial dynamics at the initial stages of soil development in glacial forefields do not contribute to
742 significant accumulation of organic carbon due to the very low growth efficiency of the microbial
743 community, resulting in a net efflux of CO_2 from those habitats. However, the low bacterial growth
744 efficiency in glacial forefields is also responsible for high rates of nutrient remineralization that most
745 probably has an important role on the establishment of plants at older ages. The relative importance of
746 allochthonous versus autochthonous substrate and nutrients is the focus of future research.

747

748 This exercise shows how an integrated model-data approach can improve understanding and
749 predictions of microbial dynamics in forefield soils and disentangle complex process interactions to
750 ascertain the relative importance of each process independently. This would, for annual budgets, be
751 extremely challenging with a purely empirical approach. Nevertheless, more clarity and data are needed
752 in tracing the dynamics and interactions of these carbon pools to improve confidence and validate model
753 simulations. Proglacial zones are expanding due to accelerated ice retreat. Thus, glacier forefields are
754 becoming an increasingly important novel habitat for microorganisms in glaciated regions experiencing
755 rapid changes in climate. This combined approach explored detailed microbial and biogeochemical

756 dynamics of soil development with the view to obtaining a more holistic picture of soil development in a
757 warmer and increasingly ice-free future world.

758

759 **Acknowledgements**

760 We thank Siegrid Debatin, Marion Maturilli, and Julia Boike (AWI) for support in acquiring meteorological
761 and radiation data, Simon Cobb, ~~and~~ James Williams, [Jane Coghill and Christy Waterfall](#) (University of
762 Bristol) for laboratory assistance, and Nicholas Cox and James Wake for assistance in the field and
763 use of the UK Station Arctic Research base in Ny-Ålesund. We also thank [Arwyn Edwards](#)
764 [\(Aberystwyth University\)](#) and ~~three~~~~two~~ anonymous referees who provided valuable comments
765 on the manuscript. This research was supported by NERC grant no. NE/J02399X/1 to A. M. Anesio. S.
766 Arndt acknowledges support from NERC grant no. NE/IO21322/1.

767

768

769 **References**

- 770 ACIA: Arctic Climate Impacts Assessment, Cambridge University Press, Cambridge, 1042,
771 2005.
- 772 Alves, R. J. E., Wanek, W., Zappe, A., Richter, A., Svenning, M. M., Schleper, C., and Urich, T.:
773 Nitrification rates in Arctic soils are associated with functionally distinct populations of
774 ammonia-oxidizing archaea, *Isme J*, 7, 1620-1631, 10.1038/ismej.2013.35, 2013.
- 775 Anderson, S. P., Drever, J. I., Frost, C. D., and Holden, P.: Chemical weathering in the foreland
776 of a retreating glacier, *Geochim Cosmochim Acta*, 64, 1173-1189, Doi 10.1016/S0016-
777 7037(99)00358-0, 2000.
- 778 Anesio, A. M., Sattler, B., Foreman, C., Telling, J., Hodson, A., Tranter, M., and Psenner, R.:
779 Carbon fluxes through bacterial communities on glacier surfaces, *Ann Glaciol*, 51, 32-40, 2010.
- 780 Bekku, Y. S., Nakatsubo, T., Kume, A., and Koizumi, H.: Soil microbial biomass, respiration rate,
781 and temperature dependence on a successional glacier foreland in Ny-Alesund, Svalbard, *Arct*
782 *Antarct Alp Res*, 36, 395-399, 2004.
- 783 Bernasconi, S. M., Bauder, A., Bourdon, B., Brunner, I., Bunemann, E., Christl, I., Derungs, N.,
784 Edwards, P., Farinotti, D., Frey, B., Frossard, E., Furrer, G., Gierga, M., Goransson, H., Gulland,
785 K., Hagedorn, F., Hajdas, I., Hindshaw, R., Ivy-Ochs, S., Jansa, J., Jonas, T., Kiczka, M.,
786 Kretzschmar, R., Lemarchand, E., Luster, J., Magnusson, J., Mitchell, E. A. D., Venterink, H. O.,
787 Plotze, M., Reynolds, B., Smittenberg, R. H., Stahli, M., Tamburini, F., Tipper, E. T., Wacker, L.,
788 Welc, M., Wiederhold, J. G., Zeyer, J., Zimmermann, S., and Zumsteg, A.: Chemical and
789 Biological Gradients along the Damma Glacier Soil Chronosequence, Switzerland, *Vadose*
790 *Zone J*, 10, 867-883, Doi 10.2136/Vzj2010.0129, 2011.
- 791 Berner, R. A., Lasaga, A. C., and Garrels, R. M.: The Carbonate-Silicate Geochemical Cycle and
792 Its Effect on Atmospheric Carbon-Dioxide over the Past 100 Million Years, *Am J Sci*, 283, 641-
793 683, 1983.
- 794 Bjorkman, M. P., Kuhnelt, R., Partridge, D. G., Roberts, T. J., Aas, W., Mazzola, M., Viola, A.,
795 Hodson, A., Strom, J., and Isaksson, E.: Nitrate dry deposition in Svalbard, *Tellus B*, 65, Art n
796 19071
797 Doi 10.3402/Tellusb.V65i0.19071, 2013.
- 798 Blagodatsky, S. A., and Richter, O.: Microbial growth in soil and nitrogen turnover: A
799 theoretical model considering the activity state of microorganisms, *Soil Biol Biochem*, 30,
800 1743-1755, Doi 10.1016/S0038-0717(98)00028-5, 1998.

801 Blagodatsky, S. A., Yevdokimov, I. V., Larionova, A. A., and Richter, J.: Microbial growth in soil
802 and nitrogen turnover: Model calibration with laboratory data, *Soil Biol Biochem*, 30, 1757-
803 1764, Doi 10.1016/S0038-0717(98)00029-7, 1998.

804 Borin, S., Ventura, S., Tambone, F., Mapelli, F., Schubotz, F., Brusetti, L., Scaglia, B., D'Acqui,
805 L. P., Solheim, B., Turicchia, S., Marasco, R., Hinrichs, K. U., Baldi, F., Adani, F., and Daffonchio,
806 D.: Rock weathering creates oases of life in a High Arctic desert, *Environ Microbiol*, 12, 293-
807 303, DOI 10.1111/j.1462-2920.2009.02059.x, 2010.

808 Boyd, E. S., Hamilton, T. L., Havig, J. R., Skidmore, M. L., and Shock, E. L.: Chemolithotrophic
809 Primary Production in a Subglacial Ecosystem, *Appl Environ Microb*, 80, 6146-6153,
810 10.1128/Aem.01956-14, 2014.

811 Bradley, J. A., Singarayer, J. S., and Anesio, A. M.: Microbial community dynamics in the
812 forefield of glaciers, *Proceedings. Biological sciences / The Royal Society*, 281, 2793-2802,
813 10.1098/rspb.2014.0882, 2014.

814 Bradley, J. A., Anesio, A. M., Singarayer, J. S., Heath, M. R., and Arndt, S.: SHIMMER (1.0): a
815 novel mathematical model for microbial and biogeochemical dynamics in glacier forefield
816 ecosystems, *Geosci. Model Dev.*, 8, 3441-3470, 10.5194/gmd-8-3441-2015, 2015.

817 Bradley, J. A., Anesio, A., and Arndt, S.: Bridging the divide: a model-data approach to Polar &
818 Alpine Microbiology, *Fems Microbiol Ecol*, 92, 10.1093/femsec/fiw015, 2016.

819 Bratbak, G., and Dundas, I.: Bacterial Dry-Matter Content and Biomass Estimations, *Appl*
820 *Environ Microb*, 48, 755-757, 1984.

821 Brown, S. P., and Jumpponen, A.: Contrasting primary successional trajectories of fungi and
822 bacteria in retreating glacier soils, *Mol Ecol*, 23, 481-497, Doi 10.1111/Mec.12487, 2014.

823 Caporaso, J. G., Kuczynski, J., Stombaugh, J., Bittinger, K., Bushman, F. D., Costello, E. K., Fierer,
824 N., Pena, A. G., Goodrich, J. K., Gordon, J. I., Huttley, G. A., Kelley, S. T., Knights, D., Koenig, J.
825 E., Ley, R. E., Lozupone, C. A., McDonald, D., Muegge, B. D., Pirrung, M., Reeder, J., Sevinsky,
826 J. R., Tumbaugh, P. J., Walters, W. A., Widmann, J., Yatsunencko, T., Zaneveld, J., and Knight,
827 R.: QIIME allows analysis of high-throughput community sequencing data, *Nat Methods*, 7,
828 335-336, 10.1038/nmeth.f.303, 2010.

829 Caporaso, J. G., Lauber, C. L., Walters, W. A., Berg-Lyons, D., Huntley, J., Fierer, N., Owens, S. M.,
830 Betley, J., Fraser, L., Bauer, M., Gormley, N., Gilbert, J. A., Smith, G., Knight, R.: Ultra-high-
831 throughput microbial community analysis on the Illumina HiSeq and MiSeq platforms, *ISME J*, 2012

832 Cary, S. C., McDonald, I. R., Barrett, J. E., and Cowan, D. A.: On the rocks: the microbiology of
833 Antarctic Dry Valley soils, *Nat Rev Microbiol*, 8, 129-138, 10.1038/nrmicro2281, 2010.

834 Darrah, P. R.: Models of the Rhizosphere .1. Microbial-Population Dynamics around a Root
835 Releasing Soluble and Insoluble Carbon, *Plant Soil*, 133, 187-199, Doi 10.1007/Bf00009191,
836 1991.

837 Dessert, C., Dupre, B., Gaillardet, J., Francois, L. M., and Allegre, C. J.: Basalt weathering laws
838 and the impact of basalt weathering on the global carbon cycle, *Chem Geol*, 202, 257-273,
839 DOI 10.1016/j.chemgeo.2002.10.001, 2003.

840 Duc, L., Noll, M., Meier, B. E., Burgmann, H., and Zeyer, J.: High Diversity of Diazotrophs in the
841 Forefield of a Receding Alpine Glacier, *Microbiol Ecol*, 57, 179-190, DOI 10.1007/s00248-008-
842 9408-5, 2009.

843 Dyurgerov, M. B., and Meier, M. F.: Twentieth century climate change: Evidence from small
844 glaciers, *P Natl Acad Sci USA*, 97, 1406-1411, DOI 10.1073/pnas.97.4.1406, 2000.

845 Edgar, R. C., Haas, B. J., Clemente, J. C., Quince, C., and Knight, R.: UCHIME improves sensitivity
846 and speed of chimera detection, *Bioinformatics*, 27, 2194-2200,
847 10.1093/bioinformatics/btr381, 2011.

848 Ensign, K. L., Webb, E. A., and Longstaffe, F. J.: Microenvironmental and seasonal variations
849 in soil water content of the unsaturated zone of a sand dune system at Pinery Provincial Park,
850 Ontario, Canada, *Geoderma*, 136, 788-802, DOI 10.1016/j.geoderma.2006.06.009, 2006.

851 Esperschütz, J., Perez-de-Mora, A., Schreiner, K., Welzl, G., Buegger, F., Zeyer, J., Hagedorn,
852 F., Munch, J. C., and Schloter, M.: Microbial food web dynamics along a soil chronosequence
853 of a glacier forefield, *Biogeosciences*, 8, 3283-3294, DOI 10.5194/bg-8-3283-2011, 2011.

854 Fleming, K. M., Dowdeswell, J. A., and Oerlemans, J.: Modelling the mass balance of northwest
855 Spitsbergen glaciers and responses to climate change, *Annals of Glaciology*, Vol 24, 1997, 24,
856 203-210, 1997.

857 Foereid, B., and Yearsley, J. M.: Modelling the impact of microbial grazers on soluble
858 rhizodeposit turnover, *Plant Soil*, 267, 329-342, DOI 10.1007/s11104-005-0139-9, 2004.

859 Frey, B., Rieder, S. R., Brunner, I., Plotze, M., Koetzsch, S., Lapanje, A., Brandl, H., and Furrer,
860 G.: Weathering-Associated Bacteria from the Damma Glacier Forefield: Physiological
861 Capabilities and Impact on Granite Dissolution, *Appl Environ Microb*, 76, 4788-4796, Doi
862 10.1128/Aem.00657-10, 2010.

863 Frey, B., Buhler, L., Schmutz, S., Zumsteg, A., and Furrer, G.: Molecular characterization of
864 phototrophic microorganisms in the forefield of a receding glacier in the Swiss Alps, *Environ*
865 *Res Lett*, 8, Artn 015033
866 Doi 10.1088/1748-9326/8/1/015033, 2013.

867 Galloway, J. N., Townsend, A. R., Erisman, J. W., Bekunda, M., Cai, Z. C., Freney, J. R.,
868 Martinelli, L. A., Seitzinger, S. P., and Sutton, M. A.: Transformation of the nitrogen cycle:
869 Recent trends, questions, and potential solutions, *Science*, 320, 889-892,
870 10.1126/science.1136674, 2008.

871 Geng, L., Alexander, B., Cole-Dai, J., Steig, E. J., Savarino, J., Sofen, E. D., and Schauer, A. J.:
872 Nitrogen isotopes in ice core nitrate linked to anthropogenic atmospheric acidity change, *P*
873 *Natl Acad Sci USA*, 111, 5808-5812, 10.1073/pnas.1319441111, 2014.

874 Goransson, H., Venterink, H. O., and Baath, E.: Soil bacterial growth and nutrient limitation
875 along a chronosequence from a glacier forefield, *Soil Biol Biochem*, 43, 1333-1340, DOI
876 10.1016/j.soilbio.2011.03.006, 2011.

877 Guelland, K., Esperschütz, J., Bornhauser, D., Bernasconi, S. M., Kretzschmar, R., and
878 Hagedorn, F.: Mineralisation and leaching of C from C-13 labelled plant litter along an initial
879 soil chronosequence of a glacier forefield, *Soil Biol Biochem*, 57, 237-247, DOI
880 10.1016/j.soilbio.2012.07.002, 2013a.

881 Guelland, K., Hagedorn, F., Smittenberg, R. H., Goransson, H., Bernasconi, S. M., Hajdas, I.,
882 and Kretzschmar, R.: Evolution of carbon fluxes during initial soil formation along the forefield
883 of Damma glacier, Switzerland, *Biogeochemistry*, 113, 545-561, DOI 10.1007/s10533-012-
884 9785-1, 2013b.

885 Hamilton, T. L., Peters, J. W., Skidmore, M. L., and Boyd, E. S.: Molecular evidence for an active
886 endogenous microbiome beneath glacial ice, *Isme J*, 7, 1402-1412, 10.1038/ismej.2013.31,
887 2013.

888 Hellweger, F. L., and Bucci, V.: A bunch of tiny individuals-Individual-based modeling for
889 microbes, *Ecol Model*, 220, 8-22, DOI 10.1016/j.ecolmodel.2008.09.004, 2009.

890 Hodkinson, I. D., Coulson, S. J., and Webb, N. R.: Community assembly along proglacial
891 chronosequences in the high Arctic: vegetation and soil development in north-west Svalbard,
892 *J Ecol*, 91, 651-663, DOI 10.1046/j.1365-2745.2003.00786.x, 2003.

893 Hodson, A., Anesio, A. M., Ng, F., Watson, R., Quirk, J., Irvine-Fynn, T., Dye, A., Clark, C.,
894 McCloy, P., Kohler, J., and Sattler, B.: A glacier respire: Quantifying the distribution and

895 respiration CO₂ flux of cryoconite across an entire Arctic supraglacial ecosystem, *J Geophys*
896 *Res-Biogeophys*, 112, Artn G04s36
897 Doi 10.1029/2007jg000452, 2007.

898 Hodson, A., Roberts, T. J., Engvall, A. C., Holmen, K., and Mumford, P.: Glacier ecosystem
899 response to episodic nitrogen enrichment in Svalbard, European High Arctic,
900 *Biogeochemistry*, 98, 171-184, DOI 10.1007/s10533-009-9384-y, 2010.

901 Hodson, A. J., Mumford, P. N., Kohler, J., and Wynn, P. M.: The High Arctic glacial ecosystem:
902 new insights from nutrient budgets, *Biogeochemistry*, 72, 233-256, DOI 10.1007/s10533-004-
903 0362-0, 2005.

904 Ingwersen, J., Poll, C., Streck, T., and Kandeler, E.: Micro-scale modelling of carbon turnover
905 driven by microbial succession at a biogeochemical interface, *Soil Biol Biochem*, 40, 864-878,
906 DOI 10.1016/j.soilbio.2007.10.018, 2008.

907 Insam, H., and Haselwandter, K.: Metabolic Quotient of the Soil Microflora in Relation to Plant
908 Succession, *Oecologia*, 79, 174-178, Doi 10.1007/Bf00388474, 1989.

909 Jakubas, D., Zmudczynska, K., Wojczulanis-Jakubas, K., and Stempniewicz, L.: Faeces
910 deposition and numbers of vertebrate herbivores in the vicinity of planktivorous and
911 piscivorous seabird colonies in Hornsund, Spitsbergen, *Pol Polar Res*, 29, 45-58, 2008.

912 Jessup, C. M., Kassen, R., Forde, S. E., Kerr, B., Buckling, A., Rainey, P. B., and Bohannan, B. J.
913 M.: Big questions, small worlds: microbial model systems in ecology, *Trends Ecol Evol*, 19,
914 189-197, 10.1016/j.tree.2004.01.008, 2004.

915 Johannessen, O. M., Bengtsson, L., Miles, M. W., Kuzmina, S. I., Semenov, V. A., Alekseev, G.
916 V., Nagurnyi, A. P., Zakharov, V. F., Bobylev, L. P., Pettersson, L. H., Hasselmann, K., and Cattle,
917 A. P.: Arctic climate change: observed and modelled temperature and sea-ice variability,
918 *Tellus A*, 56, 328-341, DOI 10.1111/j.1600-0870.2004.00060.x, 2004.

919 Kastovska, K., Elster, J., Stibal, M., and Santruckova, H.: Microbial assemblages in soil microbial
920 succession after glacial retreat in Svalbard (high Arctic), *Microbial Ecol*, 50, 396-407, DOI
921 10.1007/s00248-005-0246-4, 2005.

922 King, A. J., Meyer, A. F., and Schmidt, S. K.: High levels of microbial biomass and activity in
923 unvegetated tropical and temperate alpine soils, *Soil Biol Biochem*, 40, 2605-2610, DOI
924 10.1016/j.soilbio.2008.06.026, 2008.

925 Kirchman, D.: Measuring Bacterial Biomass Production and Growth Rates from Leucine
926 Incorporation in Natural Aquatic Environments in: *Marine Microbiology*, edited by: Paul, J. H.,
927 Academic Press, London, UK, 2001.

928 Knapp, E. B., Elliott, L. F., and Campbell, G. S.: Carbon, Nitrogen and Microbial Biomass
929 Interrelationships during the Decomposition of Wheat Straw - a Mechanistic Simulation-
930 Model, *Soil Biol Biochem*, 15, 455-461, Doi 10.1016/0038-0717(83)90011-1, 1983.

931 Kuhnel, R., Roberts, T. J., Bjorkman, M. P., Isaksson, E., Aas, W., Holmen, K., and Strom, J.: 20-
932 Year Climatology of NO₃⁻ and NH₄⁺ Wet Deposition at Ny-Alesund, Svalbard, *Adv Meteorol*,
933 Artn 406508
934 Doi 10.1155/2011/406508, 2011.

935 Kuhnel, R., Bjorkman, M. P., Vega, C. P., Hodson, A., Isaksson, E., and Strom, J.: Reactive
936 nitrogen and sulphate wet deposition at Zeppelin Station, Ny-Alesund, Svalbard, *Polar Res*,
937 32, Unsp 19136
938 Doi 10.3402/Polar.V32i0.19136, 2013.

939 Larsen, P., Hamada, Y., and Gilbert, J.: Modeling microbial communities: Current, developing,
940 and future technologies for predicting microbial community interaction, *J Biotechnol*, 160, 17-
941 24, 10.1016/j.jbiotec.2012.03.009, 2012.

942 Lazzaro, A., Brankatschk, R., and Zeyer, J.: Seasonal dynamics of nutrients and bacterial
943 communities in unvegetated alpine glacier forefields, *Appl Soil Ecol*, 53, 10-22, DOI
944 10.1016/j.apsoil.2011.10.013, 2012.

945 Lazzaro, A., Hilfiker, D., and Zeyer, J.: Structures of Microbial Communities in Alpine Soils:
946 Seasonal and Elevational Effects, *Frontiers in microbiology*, 6, ARTN 1330
947 10.3389/fmicb.2015.01330, 2015.

948 Lee, S.: A theory for polar amplification from a general circulation perspective, *Asia-Pac J*
949 *Atmos Sci*, 50, 31-43, DOI 10.1007/s13143-014-0024-7, 2014.

950 Luoto, T. P., Oksman, M., and Ojala, A. E. K.: Climate change and bird impact as drivers of High
951 Arctic pond deterioration, *Polar Biol*, 38, 357-368, 10.1007/s00300-014-1592-9, 2015.

952 Lutz, S., Anesio, A. M., Villar, S. E. J., and Benning, L. G.: Variations of algal communities cause
953 darkening of a Greenland glacier, *Fems Microbiol Ecol*, 89, 402-414, 10.1111/1574-
954 6941.12351, 2014.

955 Lutz, S., Anesio, A. M., Edwards, A., and Benning, L. G.: Microbial diversity on Icelandic glaciers
956 and ice caps, *Frontiers in microbiology*, 6, ARTN 307
957 10.3389/fmicb.2015.00307, 2015.

958 Manzoni, S., Porporato, A., D'Odorico, P., Laio, F., and Rodriguez-Iturbe, I.: Soil nutrient cycles
959 as a nonlinear dynamical system, *Nonlinear Proc Geoph*, 11, 589-598, 2004.

960 Manzoni, S., and Porporato, A.: A theoretical analysis of nonlinearities and feedbacks in soil
961 carbon and nitrogen cycles, *Soil Biol Biochem*, 39, 1542-1556, 10.1016/j.soilbio.2007.01.006,
962 2007.

963 Mapelli, F., Marasco, R., Rizzi, A., Baldi, F., Ventura, S., Daffonchio, D., and Borin, S.: Bacterial
964 Communities Involved in Soil Formation and Plant Establishment Triggered by Pyrite
965 Bioweathering on Arctic Moraines, *Microbial Ecol*, 61, 438-447, 10.1007/s00248-010-9758-7,
966 2011.

967 McDonald, D., Price, M. N., Goodrich, J., Nawrocki, E. P., DeSantis, T. Z., Probst, A., Andersen,
968 G. L., Knight, R., and Hugenholtz, P.: An improved Greengenes taxonomy with explicit ranks
969 for ecological and evolutionary analyses of bacteria and archaea, *Isme J*, 6, 610-618,
970 10.1038/ismej.2011.139, 2012.

971 Michelutti, N., Keatley, B. E., Brimble, S., Blais, J. M., Liu, H. J., Douglas, M. S. V., Mallory, M.
972 L., Macdonald, R. W., and Smol, J. P.: Seabird-driven shifts in Arctic pond ecosystems, *P Roy*
973 *Soc B-Biol Sci*, 276, 591-596, 10.1098/rspb.2008.1103, 2009.

974 Michelutti, N., Mallory, M. L., Blais, J. M., Douglas, M. S. V., and Smol, J. P.: Chironomid
975 assemblages from seabird-affected High Arctic ponds, *Polar Biol*, 34, 799-812,
976 10.1007/s00300-010-0934-5, 2011.

977 Mindl, B., Anesio, A. M., Meirer, K., Hodson, A. J., Laybourn-Parry, J., Sommaruga, R., and
978 Sattler, B.: Factors influencing bacterial dynamics along a transect from supraglacial runoff to
979 proglacial lakes of a high Arctic glacier (vol 7, pg 307, 2007), *Fems Microbiol Ecol*, 59, 762-
980 762, DOI 10.1111/j.1574-6941.2007.00295.x, 2007.

981 Moe, B., Stempniewicz, L., Jakubas, D., Angelier, F., Chastel, O., Dinessen, F., Gabrielsen, G.
982 W., Hanssen, F., Karnovsky, N. J., Ronning, B., Welcker, J., Wojczulanis-Jakubas, K., and Bech,
983 C.: Climate change and phenological responses of two seabird species breeding in the high-
984 Arctic, *Mar Ecol Prog Ser*, 393, 235-246, 10.3354/meps08222, 2009.

985 Moreau, M., Mercier, D., Laffly, D., and Roussel, E.: Impacts of recent paraglacial dynamics on
986 plant colonization: A case study on Midtre Lovénbreen foreland, Spitsbergen (79 degrees N),
987 *Geomorphology*, 95, 48-60, DOI 10.1016/j.geomorph.2006.07.031, 2008.

988 Moritz, R. E., Bitz, C. M., and Steig, E. J.: Dynamics of recent climate change in the Arctic,
989 *Science*, 297, 1497-1502, DOI 10.1126/science.1076522, 2002.

990 Paul, F., Frey, H., and Le Bris, R.: A new glacier inventory for the European Alps from Landsat
991 TM scenes of 2003: challenges and results, *Ann Glaciol*, 52, 144-152, 2011.

992 Prietzel, J., Dumig, A., Wu, Y. H., Zhou, J., and Klysubun, W.: Synchrotron-based P K-edge
993 XANES spectroscopy reveals rapid changes of phosphorus speciation in the topsoil of two
994 glacier foreland chronosequences, *Geochim Cosmochim Acta*, 108, 154-171, DOI
995 10.1016/j.gca.2013.01.029, 2013.

996 Schipper, L. A., Hobbs, J. K., Rutledge, S., and Arcus, V. L.: Thermodynamic theory explains the
997 temperature optima of soil microbial processes and high Q(10) values at low temperatures,
998 *Global Change Biol*, 20, 3578-3586, Doi 10.1111/Gcb.12596, 2014.

999 Schloss, P. D., Westcott, S. L., Ryabin, T., Hall, J. R., Hartmann, M., Hollister, E. B., Lesniewski,
1000 R. A., Oakley, B. B., Parks, D. H., Robinson, C. J., Sahl, J. W., Stres, B., Thallinger, G. G., Van
1001 Horn, D. J., and Weber, C. F.: Introducing mothur: Open-Source, Platform-Independent,
1002 Community-Supported Software for Describing and Comparing Microbial Communities, *Appl*
1003 *Environ Microb*, 75, 7537-7541, 10.1128/Aem.01541-09, 2009.

1004 Schmidt, S. K., Reed, S. C., Nemergut, D. R., Grandy, A. S., Cleveland, C. C., Weintraub, M. N.,
1005 Hill, A. W., Costello, E. K., Meyer, A. F., Neff, J. C., and Martin, A. M.: The earliest stages of
1006 ecosystem succession in high-elevation (5000 metres above sea level), recently deglaciated
1007 soils, *P Roy Soc B-Biol Sci*, 275, 2793-2802, DOI 10.1098/rspb.2008.0808, 2008.

1008 Schostag, M., Stibal, M., Jacobsen, C. S., Baelum, J., Tas, N., Elberling, B., Jansson, J. K.,
1009 Semenchuk, P., and Prieme, A.: Distinct summer and winter bacterial communities in the
1010 active layer of Svalbard permafrost revealed by DNA- and RNA-based analyses, *Frontiers in*
1011 *microbiology*, 6, ARTN 399
1012 10.3389/fmicb.2015.00399, 2015.

1013 Schulz, S., Brankatschk, R., Dumig, A., Kogel-Knabner, I., Schloter, M., and Zeyer, J.: The role
1014 of microorganisms at different stages of ecosystem development for soil formation,
1015 *Biogeosciences*, 10, 3983-3996, DOI 10.5194/bg-10-3983-2013, 2013.

1016 Schutte, U. M. E., Abdo, Z., Bent, S. J., Williams, C. J., Schneider, G. M., Solheim, B., and Forney,
1017 L. J.: Bacterial succession in a glacier foreland of the High Arctic, *Isme J*, 3, 1258-1268, DOI
1018 10.1038/ismej.2009.71, 2009.

1019 Scott, E. M., Rattray, E. A. S., Prosser, J. I., Killham, K., Glover, L. A., Lynch, J. M., and Bazin, M.
1020 J.: A Mathematical-Model for Dispersal of Bacterial Inoculants Colonizing the Wheat
1021 Rhizosphere, *Soil Biol Biochem*, 27, 1307-1318, Doi 10.1016/0038-0717(95)00050-O, 1995.

1022 Serreze, M. C., Walsh, J. E., Chapin, F. S., Osterkamp, T., Dyurgerov, M., Romanovsky, V.,
1023 Oechel, W. C., Morison, J., Zhang, T., and Barry, R. G.: Observational evidence of recent change
1024 in the northern high-latitude environment, *Climatic Change*, 46, 159-207, Doi
1025 10.1023/A:1005504031923, 2000.

1026 Servedio, M. R., Brandvain, Y., Dhole, S., Fitzpatrick, C. L., Goldberg, E. E., Stern, C. A., Van
1027 Cleve, J., and Yeh, D. J.: Not just a theory--the utility of mathematical models in evolutionary
1028 biology, *Plos Biol*, 12, e1002017, 10.1371/journal.pbio.1002017, 2014.

1029 Simon, M., and Azam, F.: Protein-Content and Protein-Synthesis Rates of Planktonic Marine-
1030 Bacteria, *Mar Ecol Prog Ser*, 51, 201-213, DOI 10.3354/meps051201, 1989.

1031 Smittenberg, R. H., Gierga, M., Goransson, H., Christl, I., Farinotti, D., and Bernasconi, S. M.:
1032 Climate-sensitive ecosystem carbon dynamics along the soil chronosequence of the Damma
1033 glacier forefield, Switzerland, *Global Change Biol*, 18, 1941-1955, DOI 10.1111/j.1365-
1034 2486.2012.02654.x, 2012.

1035 Soetaert, K., and Herman, P.: A Practical Guide to Ecological Modelling: Using R as a Simulation
1036 Platform, Springer, UK, 2009.

1037 Staines, K. E. H., Carrivick, J. L., Tweed, F. S., Evans, A. J., Russell, A. J., Jóhannesson, T., and
1038 Roberts, M.: A multi-dimensional analysis of pro-glacial landscape change at Sólheimajökull,
1039 southern Iceland, *Earth Surface Processes and Landforms*, 40, 809-822, 10.1002/esp.3662,
1040 2014.

1041 Stapleton, L. M., Crout, N. M. J., Sawstrom, C., Marshall, W. A., Poulton, P. R., Tye, A. M., and
1042 Laybourn-Parry, J.: Microbial carbon dynamics in nitrogen amended Arctic tundra soil:
1043 Measurement and model testing, *Soil Biol Biochem*, 37, 2088-2098, DOI
1044 10.1016/j.soilbio.2005.03.016, 2005.

1045 Stibal, M., Tranter, M., Benning, L. G., and Rehak, J.: Microbial primary production on an Arctic
1046 glacier is insignificant in comparison with allochthonous organic carbon input, *Environ*
1047 *Microbiol*, 10, 2172-2178, 10.1111/j.1462-2920.2008.01620.x, 2008.

1048 Strauss, S. L., Garcia-Pichel, F., and Day, T. A.: Soil microbial carbon and nitrogen
1049 transformations at a glacial foreland on Anvers Island, Antarctic Peninsula, *Polar Biol*, 35,
1050 1459-1471, DOI 10.1007/s00300-012-1184-5, 2012.

1051 Telling, J., Anesio, A. M., Tranter, M., Irvine-Fynn, T., Hodson, A., Butler, C., and Wadham, J.:
1052 Nitrogen fixation on Arctic glaciers, Svalbard, *J Geophys Res-Biogeophys*, 116, Artn G03039
1053 Doi 10.1029/2010jg001632, 2011.

1054 Telling, J., Stibal, M., Anesio, A. M., Tranter, M., Nias, I., Cook, J., Bellas, C., Lis, G., Wadham,
1055 J. L., Sole, A., Nienow, P., and Hodson, A.: Microbial nitrogen cycling on the Greenland Ice
1056 Sheet, *Biogeosciences*, 9, 2431-2442, 10.5194/bg-9-2431-2012, 2012.

1057 Toal, M. E., Yeomans, C., Killham, K., and Meharg, A. A.: A review of rhizosphere carbon flow
1058 modelling, *Plant Soil*, 222, 263-281, Doi 10.1023/A:1004736021965, 2000.

1059 Tscherko, D., Rustemeier, J., Richter, A., Wanek, W., and Kandeler, E.: Functional diversity of
1060 the soil microflora in primary succession across two glacier forelands in the Central Alps, *Eur*
1061 *J Soil Sci*, 54, 685-696, DOI 10.1046/j.1365-2389.2003.00570.x, 2003.

1062 Vandewerf, H., and Verstraete, W.: Estimation of Active Soil Microbial Biomass by
1063 Mathematical-Analysis of Respiration Curves - Development and Verification of the Model,
1064 *Soil Biol Biochem*, 19, 253-260, Doi 10.1016/0038-0717(87)90006-X, 1987.

1065 Wang, Y. P., Chen, B. C., Wieder, W. R., Leite, M., Medlyn, B. E., Rasmussen, M., Smith, M. J.,
1066 Agosto, F. B., Hoffman, F., and Luo, Y. Q.: Oscillatory behavior of two nonlinear microbial
1067 models of soil carbon decomposition, *Biogeosciences*, 11, 1817-1831, 10.5194/bg-11-1817-
1068 2014, 2014.

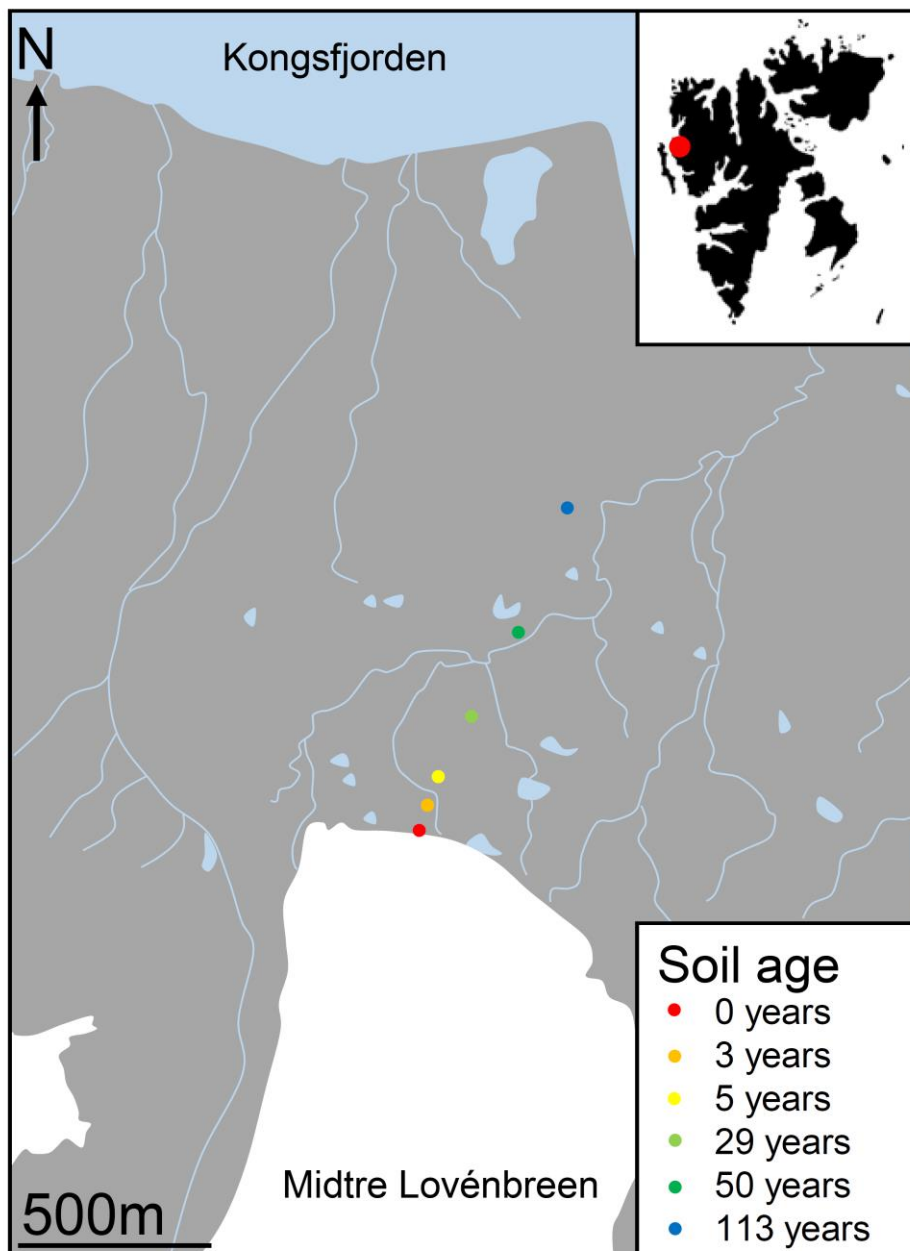
1069 Yde, J. C., Finster, K. W., Raiswell, R., Steffensen, J. P., Heinemeier, J., Olsen, J., Gunnlaugsson,
1070 H. P., and Nielsen, O. B.: Basal ice microbiology at the margin of the Greenland ice sheet, *Ann*
1071 *Glaciol*, 51, 71-79, 2010.

1072 Yoshitake, S., Uchida, M., Koizumi, H., Kanda, H., and Nakatsubo, T.: Production of biological
1073 soil crusts in the early stage of primary succession on a High Arctic glacier foreland, *New*
1074 *Phytol*, 186, 451-460, DOI 10.1111/j.1469-8137.2010.03180.x, 2010.

1075 Zdanowski, M. K., Zmuda-Baranowska, M. J., Borsuk, P., Swiatecki, A., Gorniak, D., Wolicka,
1076 D., Jankowska, K. M., and Grzesiak, J.: Culturable bacteria community development in
1077 postglacial soils of Ecology Glacier, King George Island, Antarctica, *Polar Biol*, 36, 511-527, DOI
1078 10.1007/s00300-012-1278-0, 2013.

1079 Zelenev, V. V., van Bruggen, A. H. C., and Semenov, A. M.: "BACWAVE," a spatial-temporal
1080 model for traveling waves of bacterial populations in response to a moving carbon source in
1081 soil, *Microbial Ecol*, 40, 260-272, 2000.

1082 Zhang, X. Y., Wang, W., Chen, W. L., Zhang, N. L., and Zeng, H.: Comparison of Seasonal Soil
1083 Microbial Process in Snow-Covered Temperate Ecosystems of Northern China, Plos One, 9,
1084 ARTN e92985
1085 10.1371/journal.pone.0092985, 2014.
1086 Ziolk, M., and Melke, J.: The impact of seabirds on the content of various forms of
1087 phosphorus in organic soils of the Bellsund coast, western Spitsbergen, Polar Res, 33, ARTN
1088 19986
1089 10.3402/polar.v33.19986, 2014.
1090 Zumsteg, A., Bernasconi, S. M., Zeyer, J., and Frey, B.: Microbial community and activity shifts
1091 after soil transplantation in a glacier forefield, Appl Geochem, 26, S326-S329, DOI
1092 10.1016/j.apgeochem.2011.03.078, 2011.
1093 Zumsteg, A., Luster, J., Goransson, H., Smittenberg, R. H., Brunner, I., Bernasconi, S. M., Zeyer,
1094 J., and Frey, B.: Bacterial, Archaeal and Fungal Succession in the Forefield of a Receding
1095 Glacier, Microbial Ecol, 63, 552-564, DOI 10.1007/s00248-011-9991-8, 2012.
1096 Zumsteg, A., Schmutz, S., and Frey, B.: Identification of biomass utilizing bacteria in a carbon-
1097 depleted glacier forefield soil by the use of ¹³C DNA stable isotope probing, Env Microbiol
1098 Rep, 5, 424-437, Doi 10.1111/1758-2229.12027, 2013.
1099
1100
1101
1102
1103
1104
1105
1106

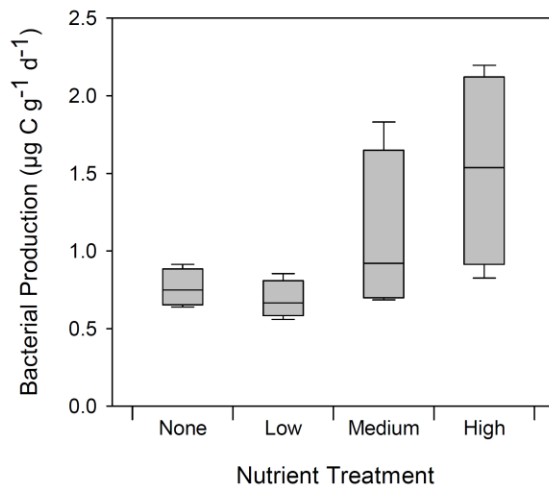


1108

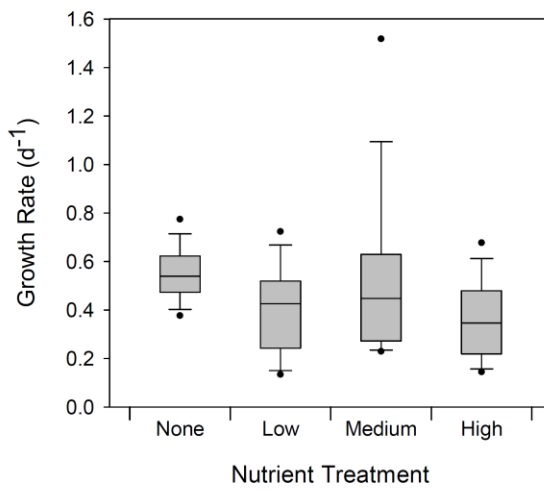
1109 Figure 1. Midtre Lovénbreen glacier and forefield in Svalbard, the location of sampling sites and
1110 approximate age of soil.

1111

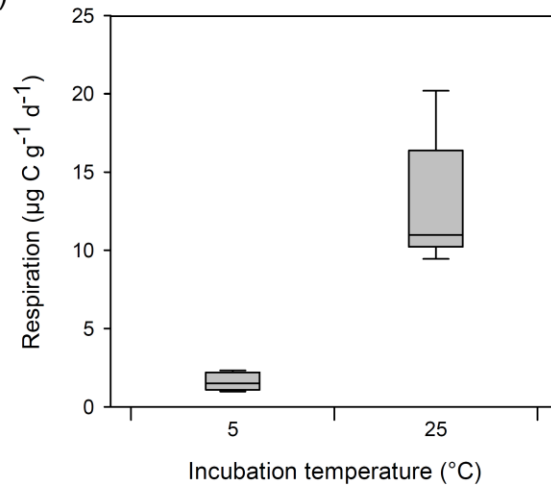
(a)



(b)



(c)



1112

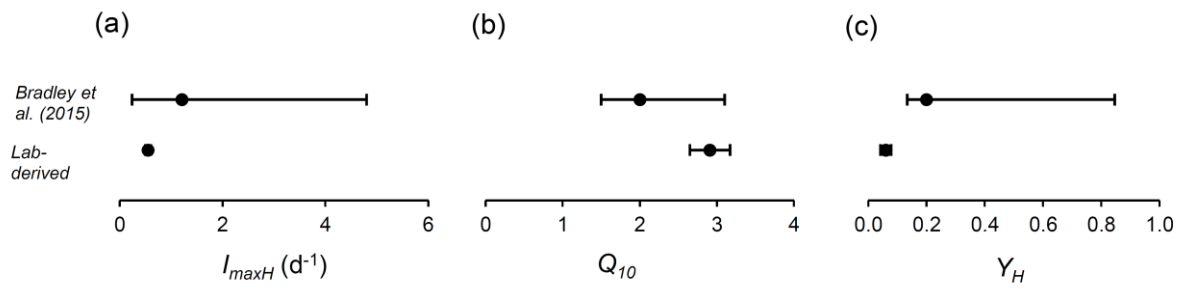
1113 Figure 2. Measurements of (a) bacterial carbon production and (b) growth rate, derived from ^3H -leucine

1114 assays at different nutrient conditions, and (c) bacterial respiration at 5°C and 25°C.

1115

1116

1117



1118

1119

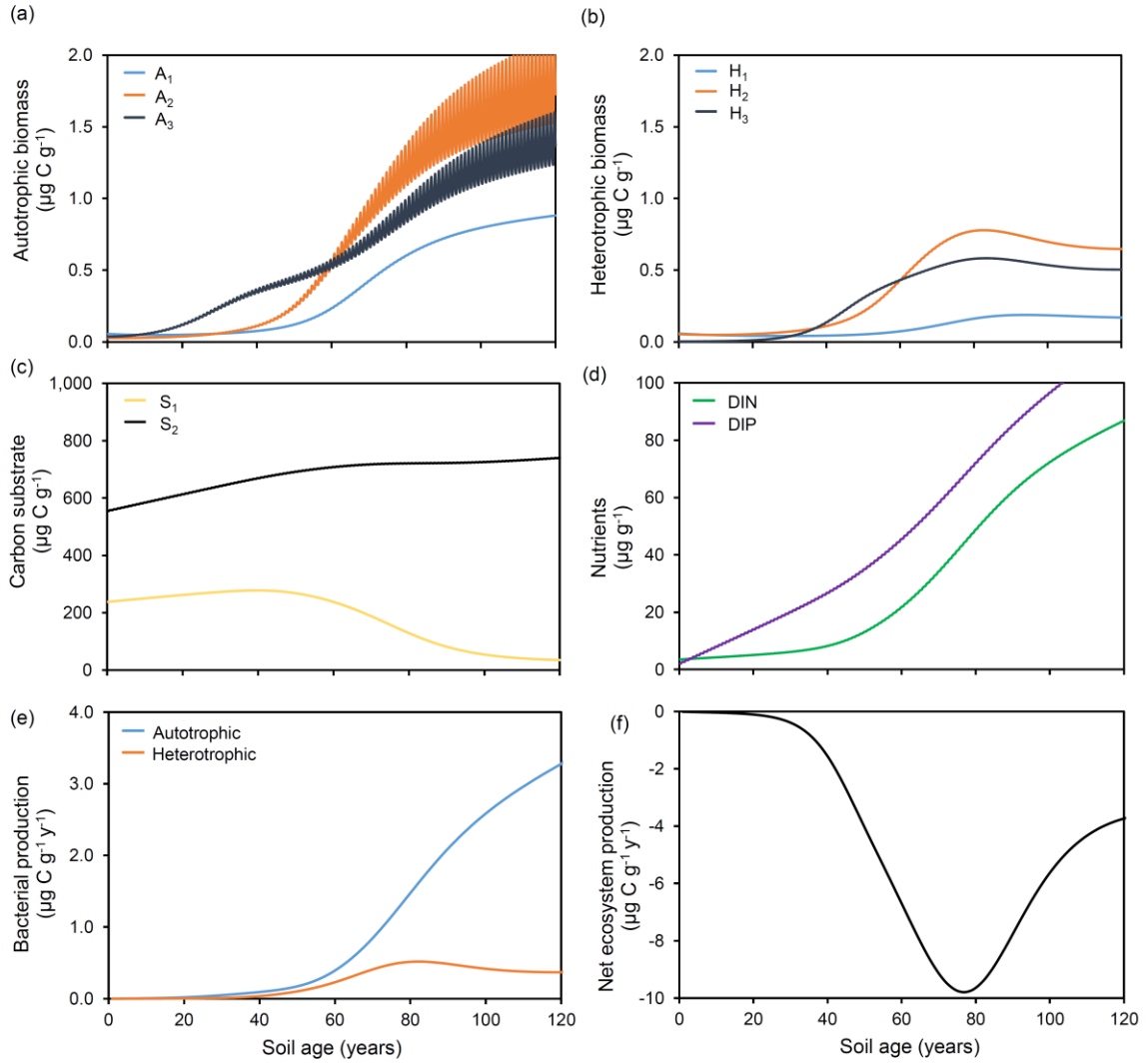
1120

1121 Figure 3. A comparison of previously established ranges for parameters (Bradley et al., 2015) with

1122 laboratory-derived values for (a) maximum growth rate (I_{max}), (b) temperature response (Q_{10}), (c) BGE

1123 (γ).

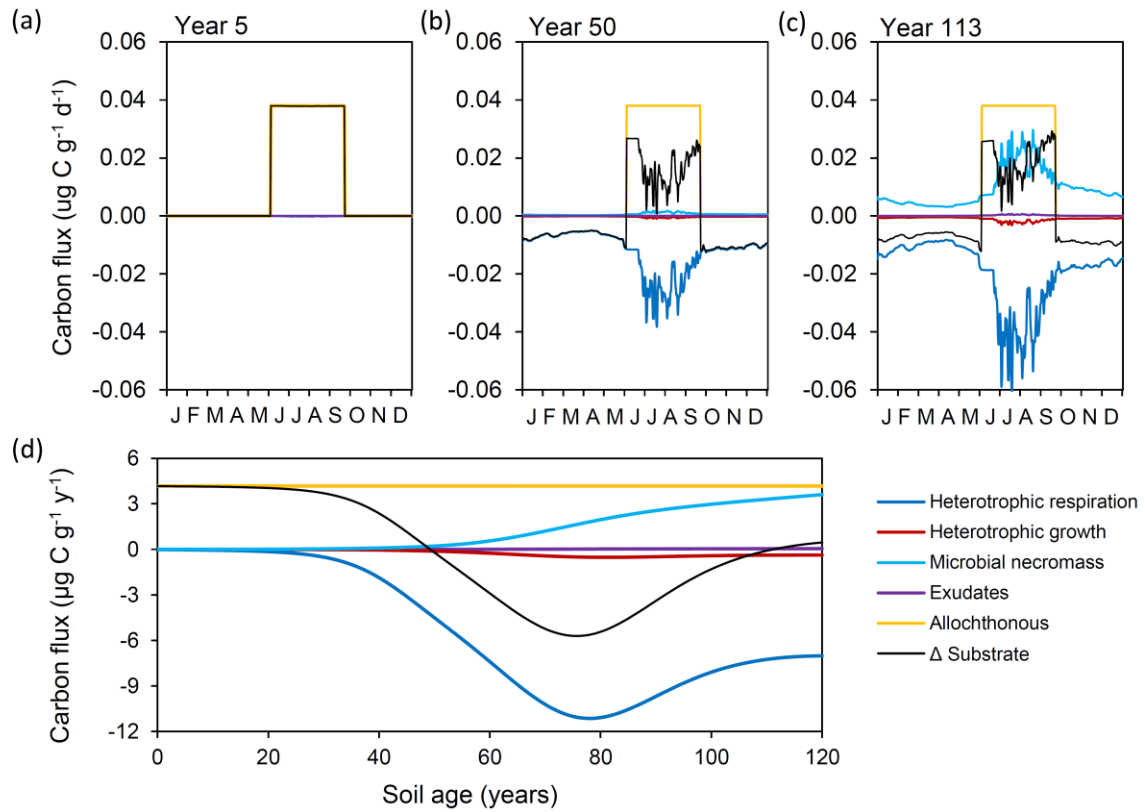
1124



1125

1126 Figure 4. Modelled (a) autotrophic biomass, (b) heterotrophic biomass, (c) carbon substrate, (d)
 1127 nutrients, (e) bacterial production and (f) net ecosystem production, with laboratory-derived parameter
 1128 values.

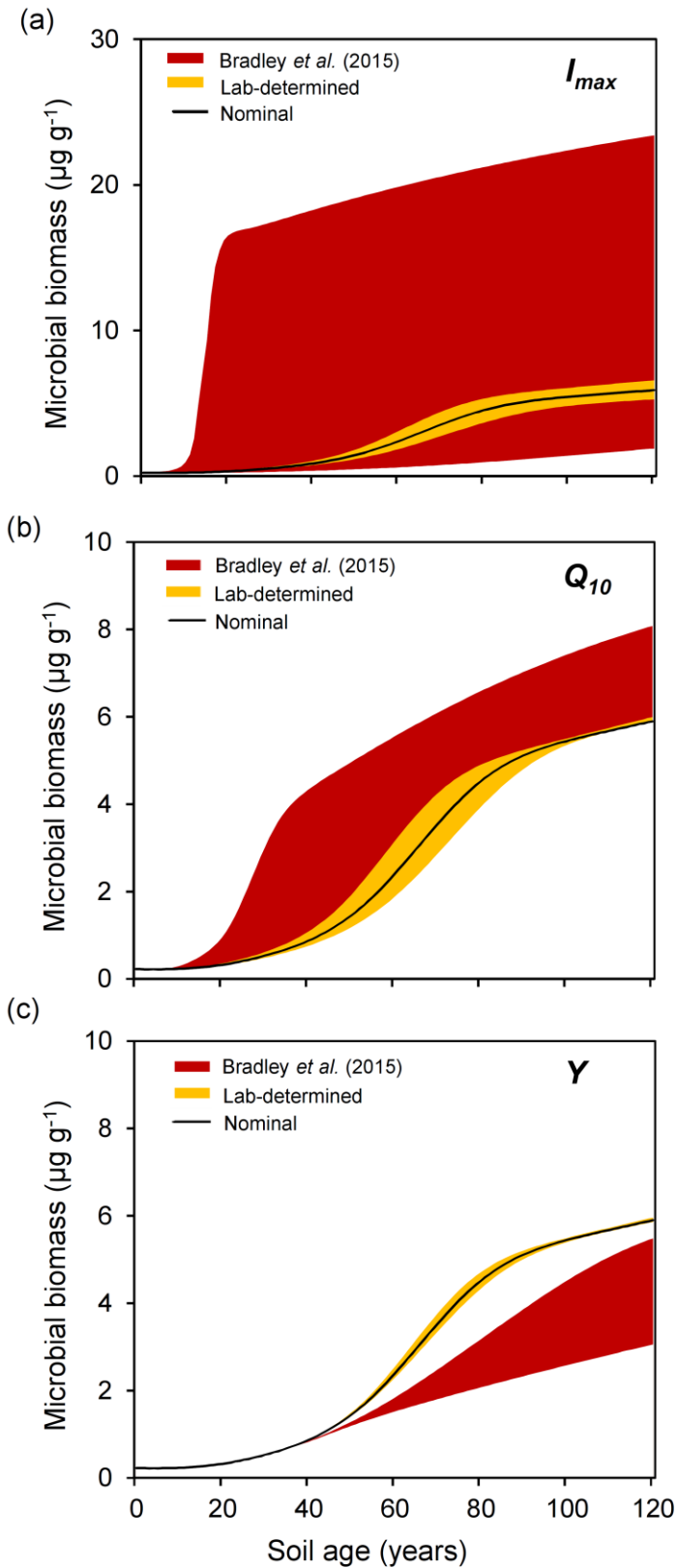
1129



1130

1131 Figure 5. Illustration of daily carbon fluxes for (a) 5, (b) 50 and (c) 113 year old soil, and (d) annual
 1132 carbon flux over 120 years. Microbial necromass (light blue), exudates (purple) and allochthonous
 1133 sources (yellow) contribute to the substrate pool (black), and heterotrophic growth (red) and respiration
 1134 (dark blue) deplete it.

1135



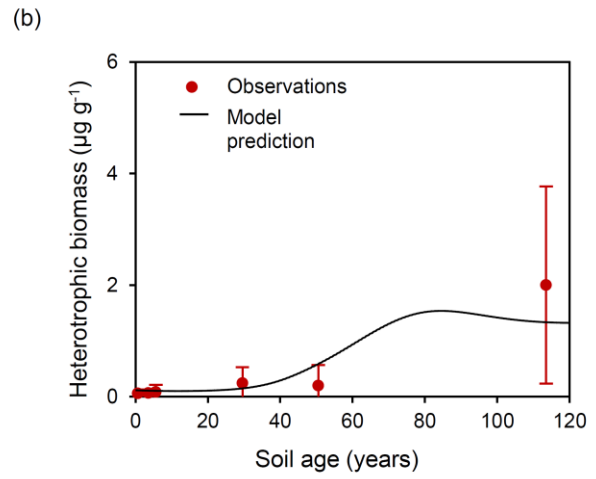
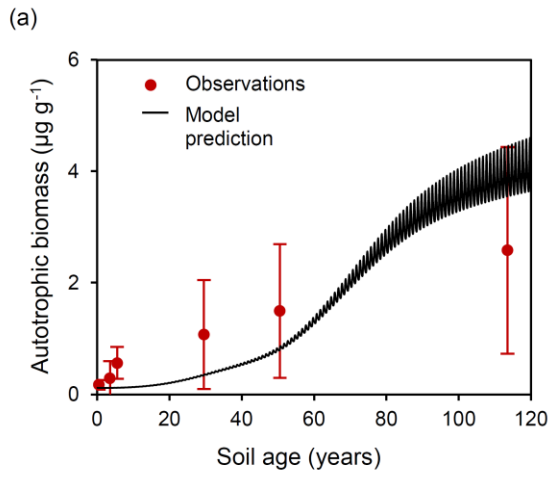
1136

1137 Figure 6. A comparison of predicted microbial biomass with laboratory-derived parameter values

1138 (yellow) and previously established parameter values (Bradley *et al.*, 2015) (red) for variation in the

1139 following parameters: (a) maximum growth rate (I_{max}), (b) temperature response (Q_{10}), (c) BGE (Y).

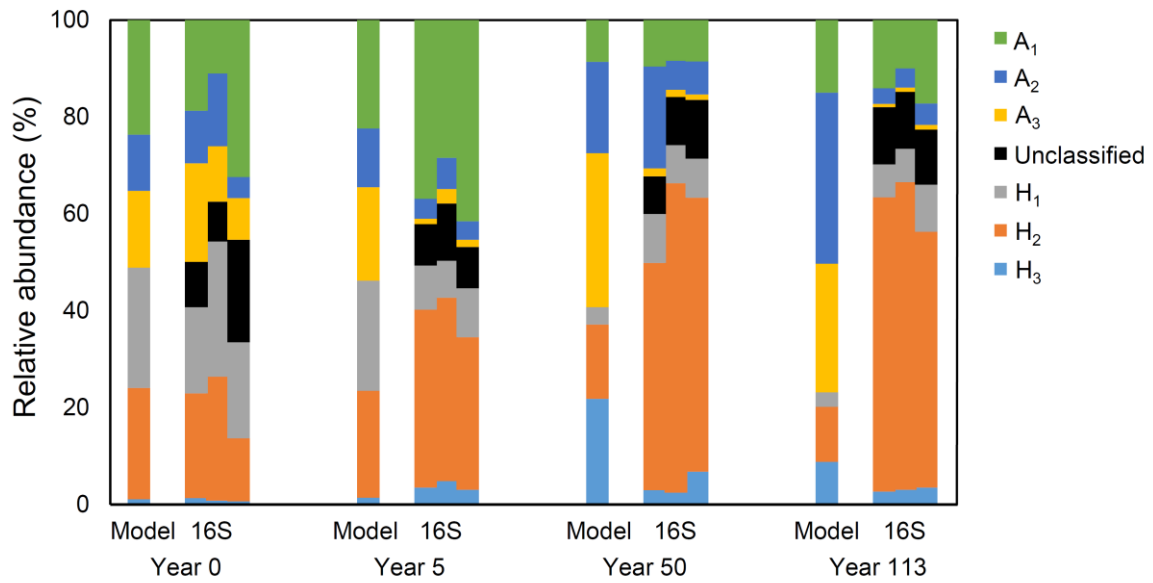
1140



1141

1142 Figure 7. Model predictions of (a) autotrophic and (b) heterotrophic biomass (black line), compared to
1143 observational data (red) derived from microscopy.

1144



1145

1146 Figure 8. A comparison of microbial diversity from model output and genomic analyses at 0 year old, 5

1147 year old, 50 year old and 113 year old soil.

1148

1149

1150

1151

1152 Table 1. State variables and initial values.

State Variable	Units	Description	Initial value (year 0) ($\mu\text{g g}^{-1}$)
A ₁	$\mu\text{g C g}^{-1}$	Glacial chemolithoautotrophs	0.0547
A ₂	$\mu\text{g C g}^{-1}$	Soil autotrophs	0.0266
A ₃	$\mu\text{g C g}^{-1}$	Nitrogen fixing soil autotrophs	0.0355
H ₁	$\mu\text{g C g}^{-1}$	Glacial heterotrophs	0.0576
H ₂	$\mu\text{g C g}^{-1}$	Soil heterotrophs	0.0530
H ₃	$\mu\text{g C g}^{-1}$	Nitrogen fixing soil heterotrophs	0.0025
S ₁	$\mu\text{g C g}^{-1}$	Labile organic carbon	291.895
S ₂	$\mu\text{g C g}^{-1}$	Refractory organic carbon	681.089
DIN	$\mu\text{g N g}^{-1}$	Dissolved inorganic nitrogen (DIN)	3.530
DIP	$\mu\text{g P g}^{-1}$	Dissolved inorganic phosphorus (DIP)	2.078
ON ₁	$\mu\text{g N g}^{-1}$	Labile organic nitrogen	41.157
ON ₂	$\mu\text{g N g}^{-1}$	Refractory organic nitrogen	96.034
OP ₁	$\mu\text{g P g}^{-1}$	Labile organic phosphorus	24.227
OP ₂	$\mu\text{g P g}^{-1}$	Refractory organic phosphorus	56.530

1153

1154

1155

1156

1157 Table 2. Microbial biomass in the forefield of Midtre Lovénbreen (brackets show 1 standard deviation)
 1158

Soil Age (years)	Autotrophic biomass ($\mu\text{g C g}^{-1}$)	Heterotrophic biomass ($\mu\text{g C g}^{-1}$)	Total Organic Carbon ($\mu\text{g C g}^{-1}$)
0	0.171 (0.042)	0.059 (0.034)	792.984 (127.206)
3	0.287 (0.155)	0.064 (0.029)	
5	0.561 (0.143)	0.083 (0.065)	
29	1.072 (0.487)	0.244 (0.142)	
50	1.497 (0.601)	0.197 (0.184)	
113	2.581 (0.927)	2.000 (0.885)	

1159
 1160
 1161
 1162
 1163
 1164

1165 Table 3. Model output.

Soil Age (years)	Autotrophic biomass ($\mu\text{g C g}^{-1}$)	Heterotrophic biomass ($\mu\text{g C g}^{-1}$)	Autotrophic production ($\mu\text{g C g}^{-1} \text{y}^{-1}$)	Heterotrophic production ($\mu\text{g C g}^{-1} \text{y}^{-1}$)	Net ecosystem production ($\mu\text{g C g}^{-1} \text{y}^{-1}$)	DIN assimilation ($\mu\text{g N g}^{-1} \text{y}^{-1}$)	N_2 fixation ($\mu\text{g N g}^{-1} \text{y}^{-1}$)
0	0.117	0.111	0.002	0.001	- 0.011	2.0×10^{-4}	2.0×10^{-4}
3	0.117	0.105	0.003	0.001	- 0.020	3.0×10^{-4}	3.0×10^{-4}
5	0.119	0.102	0.004	0.001	- 0.025	4.0×10^{-4}	4.0×10^{-4}
29	0.359	0.147	0.050	0.012	- 0.391	0.002	0.006
50	0.860	0.591	0.187	0.113	- 4.311	0.022	0.021
113	4.414	1.331	3.093	0.376	- 4.031	0.458	0.031

1166
 1167
 1168
 1169
 1170
 1171
 1172